NASA CONTRACTOR REPORT

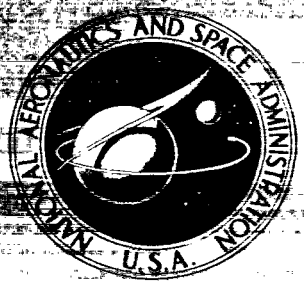

ALUMINUM CHLORINE BATTERY

by José Giner and Gerhard L. Holleck

Prepared by
TYCO LABORATORIES, INC.
Waltham, Mass.
for Electronics Research Center

NATIONAL AERONAUTICS AND SPACE ADMINISTRATION • WASHINGTON, D. C. • MARCH 1970

ALUMINUM CHLORINE BATTERY

By José Giner and Gerhard L. Holleck

Prepared under Contract No. NAS 12-688 by
TYCO LABORATORIES, INC.
Waltham, Mass.

for Electronics Research Center

NATIONAL AERONAUTICS AND SPACE ADMINISTRATION

For sale by the Clearinghouse for Federal Scientific and Technical Information
Springfield, Virginia 22151 – CFSTI price $3.00

Table of Contents

List of Illustrations

List of Illustrations (Cont.)

List of Tables

ALUMINUM CHLORINE BATTERY

By José Giner and Gerhard L. Holleck

Tyco Laboratories, Inc.
Waltham, Massachusetts 02154

SUMMARY

A molten salt system based on Al and Cl_2 carbon electrodes with an $AlCl_3$-alkali chloride eutectic as electrolyte offers promise as a rechargeable, high energy density battery which can operate at a relatively low temperature and may withstand sterilization. To obtain pure $AlCl_3$-KCl-NaCl melts, different commercial aluminum chloride materials have been investigated. $FeCl_3$ was found to be the major impurity in all of them. A procedure involving treatment of a melt of high $AlCl_3$ concentration with magnesium powder prior to evaporation yielded pure $AlCl_3$. $AlCl_3$-KCl-NaCl melts using this material stayed clear (nearly colorless), and showed practically no background current.

Investigations of vitreous carbon electrodes have shown that carbon is intrinsically active for chlorine reduction in $AlCl_3$-alkali chloride melts. A study of compatibility of carbon electrodes for chlorine in $AlCl_3$ eutectics has uncovered carbon samples which appear suited for the construction of porous chlorine cathodes.

Passivation phenomena have been observed upon cathodic and anodic polarization of the aluminum electrode in $AlCl_3$-KCl-NaCl melts. It was established that they are not due to an electrochemical (potential dependent) process, but rather are caused by formation of a solid salt layer at the electrode surface resulting from concentration changes upon anodic or cathodic current flow. The value of the steady state current is determined by diffusion processes in the melt and by the

concentration change necessary to pass the liquidus curve of the phase diagram. The electrode behavior upon cathodic polarization is further complicated by dendrite growth which causes the electrode to expand into the melt.

The feasibility of an aluminum chloride battery in the primary mode was experimentally demonstrated.

INTRODUCTION

A great deal of effort over the past 7 years has been directed toward the development of batteries with energy densities of the order of 200 W-hr/lb. The negatives in these high energy density systems are characteristically selected from the most electronegative of the metals. The use of electronegative metals such as Li or Na necessitates the use of electrolytes which are aprotic. Organic and molten salt media have both been used; however, since aprotic organic electrolytes can be used at ambient temperatures, these have received by far the greater amount of attention.

Major disadvantages of cells based on aprotic organic electrolytes are instability of positive plates (resulting in short shelf life) and low conductivity. The chief disadvantage of molten electrolyte batteries being presently investigated is the necessity for high temperature operation which introduces many problems relating to materials of construction, safety, etc. Furthermore, the insulation needed to keep these high temperature batteries in an operating condition leads to a degradation of the energy density of the battery.

It seems possible to overcome the problems associated with the high working temperatures of the present molten salt systems, while still retaining the advantages of high energy density and relatively efficient electrode processes, by using a cell composed of an Al negative and a Cl_2 positive in a low temperature electrolyte of molten $AlCl_3$-NaCl-KCl. The operating temperature of this system would be in the range 120 to 150 °C, with a theoretical energy density of 650 W-hr/lb. Furthermore, it should

be possible to obtain a cell operable at even lower temperatures by using as electrolyte a melt of $AlCl_3$ with one or more of the other alkali chlorides (LiCl, RbCl, CsCl) which are all lower melting than NaCl or KCl.

The theoretical energy density of 650 W-hr/lb for the Al-Cl_2 system compares favorably with that of 754 W-hr/lb for the Li-CuF_2 (propylene carbonate) system and 990 W-hr/lb for the Li-Cl_2 (molten salt) system. Another advantage of the Al-Cl_2 system would be that solid Al is easier to handle and much less hazardous than molten Li or Na. The hazards of the Cl_2 electrode (common to both the Li-Cl_2 and the proposed new system) will be reduced to some extent by the lower working temperatures; the same methods suggested for this electrode in the high temperature cell (adsorption and occlusion on porous carbon or graphite) can be used here.

To devise a practical, workable cell, more knowledge is required of the reactions that take place at the anode and cathode of the particular system, as well as a knowledge of the electrolyte properties and of the interaction of the complete system.

In addition to demonstrating the feasibility of this kind of battery, it is our aim to optimize it and to define its limitations by determining the kinetic parameters of the electrodes and the pertinent physico-chemical data of the electrolyte.

ALUMINUM CHLORIDE-ALKALI HALIDE MELTS

Properties of the Melts

$AlCl_3$ itself melts at a low temperature (190 °C), but has a very low conductivity [at 700 °C, $\kappa = 6.56 \times 10^{-6}\ \Omega^{-1}cm^{-1}$, and in the region of the melting point it is even lower (Ref. 1)]. However, it is possible to obtain a lower melting system with considerably increased conductivity by addition of NaCl and/or KCl.

The available data on $AlCl_3$-alkali halide eutectics are listed in Table I. It can be readily seen that much work has been done on the $AlCl_3$-NaCl, $AlCl_3$-KCl and the $AlCl_3$-NaCl-KCl mixtures. The other alkali halides, however, have received scant attention.

Thermal analyses of the $AlCl_3$-KCl-NaCl system have been carried out (Refs. 2 and 3). The complete phase diagram, taken from Ref 2, is shown in Fig. 1 and several cross sections from it are shown in Fig. 2. As can be seen from Table I, the lowest melting eutectic in the $AlCl_3$-NaCl-KCl system is formed between the intermediate compounds $KAlCl_4$, $NaAlCl_4$, and $AlCl_3$. Its melting point was reported to be 70 °C at an approximate composition of 66 mol % $AlCl_3$, 14 mol % KCl, and 20 mol % NaCl. Reference to Table I reveals that little is known about the $AlCl_3$ rich region, i. e., the low temperature region of the phase diagram. In this region, we can anticipate a rather high vapor pressure of $AlCl_3$, since not all of the $AlCl_3$ will be present as the complex $AlCl_4^-$. It has, however, been proposed (Ref. 3) that in an $AlCl_3$ rich melt the following solvation process takes place:

$$AlCl_3 + AlCl_4^- \rightleftharpoons Al_2Cl_7^-$$

Conductivity and density measurements have been carried out by Midorikawa (Ref. 18) on the ternary melt. In the temperature range 130 to 205 °C and composition range 21. 3 to 40. 4 mol % NaCl and 5. 8 to 23. 9 mol % KCl, the conductivity lies in the range 0. 365 to 0. 118 $\Omega^{-1}cm^{-1}$. The relation between κ and temperature is approximately

TABLE I
$AlCl_3$-ALKALI HALIDE EUTECTIC MELTS

System	Composition, mol %	Eutectic Melting Point, °C	Reference No.
$AlCl_3$-LiCl	60	114	10, 16
$AlCl_3$-NaCl	62	112	5, 2, 8, 4, 6, 7, 9, 10
	60	115	12, 14, 15, 16
	59	123	
	50	150	
	66	93	
$AlCl_3$-NaCl	61	108	2, 4, 16
$AlCl_3$-KCl	67	128	2, 8, 4, 1, 6, 9, 10 13, 17
$AlCl_3$-KCl	71-65.5	114-149	16
$AlCl_3$-KCl-NaCl	60-14-26	93	2, 8, 3, 9, 16
	63.5-16.5-20	88-9	
	62.13-12.7-25.17	94	
	66-14-20	70	
$AlCl_3$-RbCl			
$AlCl_3$-CsCl	74.6	148	11

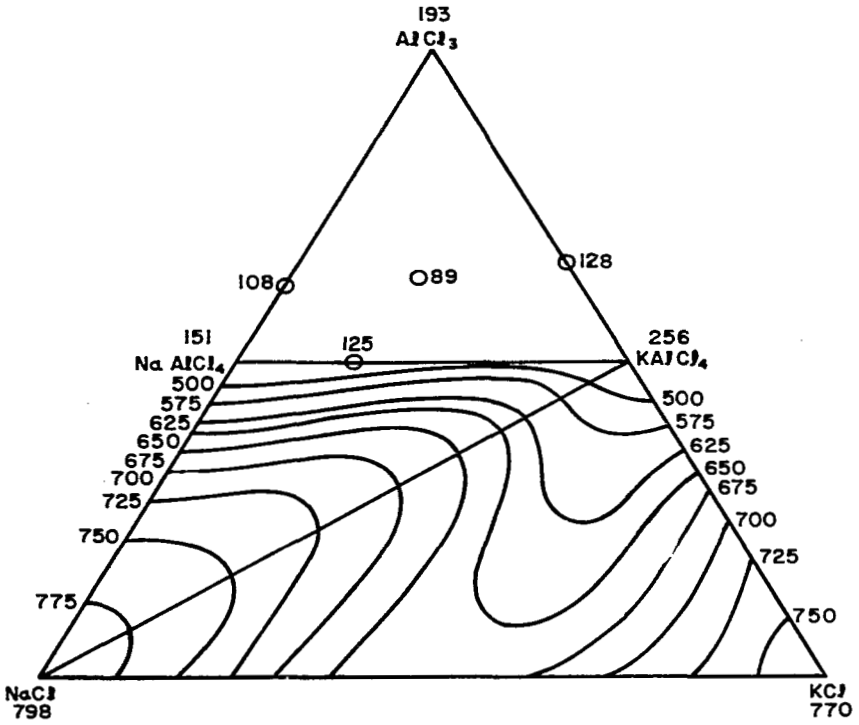

Fig. 1. Phase diagram for the system $AlCl_3$-NaCl-KCl (O = eutectics; temperature = °C; data from Fisher and Simon[2])

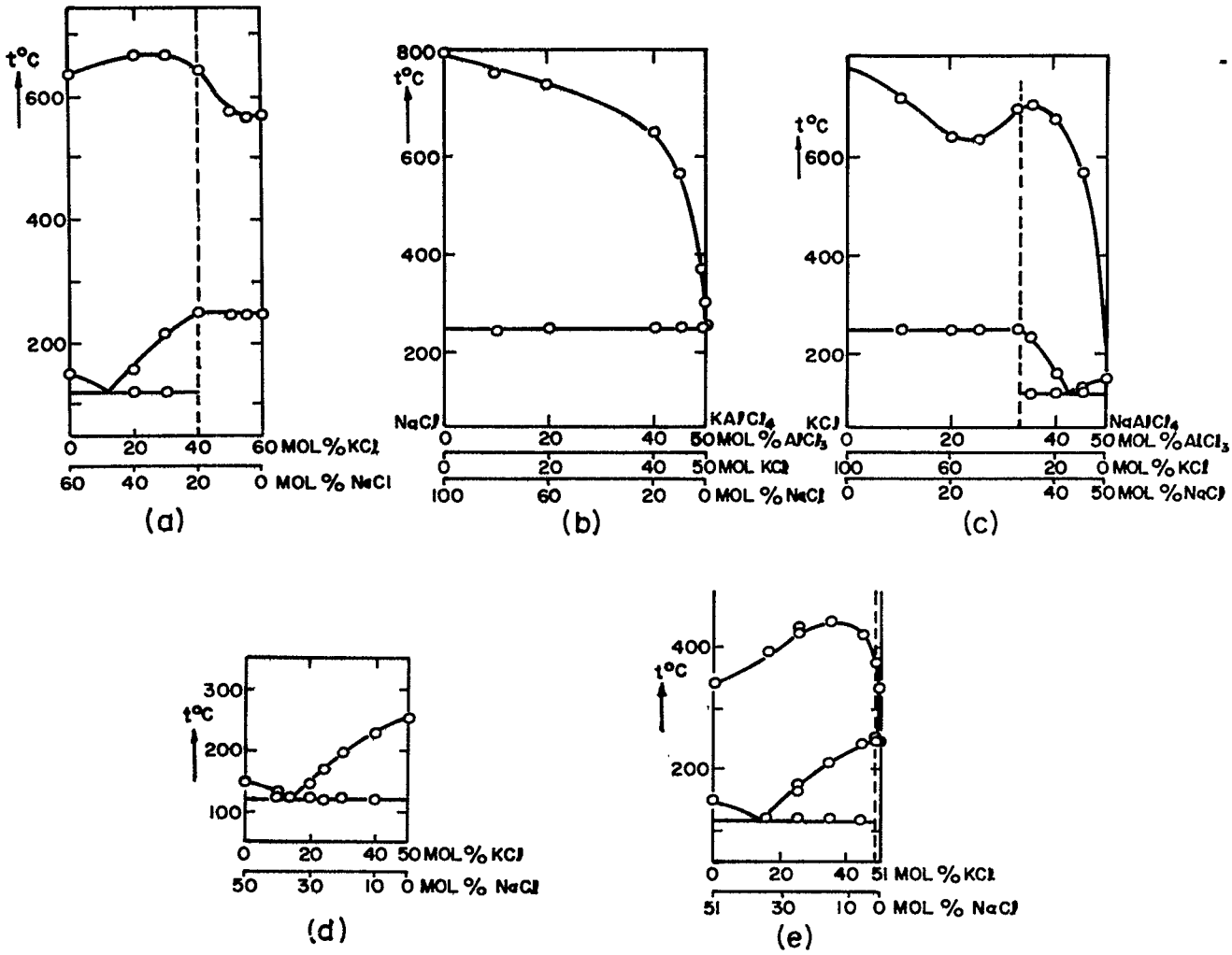

Fig. 2. Cross sections from the phase diagram for the system $AlCl_3$-NaCl-KCl

(a) Section through ternary system at 49 mol% $AlCl_3$

(b) Pseudobinary section NaCl-$KAlCl_4$

(c) Section KCl-$NaAlCl_4$

(d) Section through ternary system at 50 mol% $AlCl_3$ (pseudobinary system $NaAlCl_4$-$KAlCl_4$)

(e) Section through ternary system at 40 mol% $AlCl_3$

linear in this range. Midorikawa states that the large contribution to the conductivity of the ternary mixtures is made by NaCl; the contribution from KCl is only 50% of that made by NaCl.

Analogy with the binary melts (see above) suggests that maximum conductivity should occur at the composition $NaAlCl_4 \cdot KAlCl_4$ (i.e., 50 mol % $AlCl_3$, 25 mol % NaCl, and 25 mol % KCl).

Melts containing $AlCl_3$, NaCl, and KCl are stable. They have been used as reaction media for organic reactions [e.g., addition of KCl to C_2H_4 (Ref. 19)]. It appears that these melts can be used in Pyrex (or Vycor) glass at temperatures up to 700 °C (Refs. 2, 19, and 20). At temperatures up to 800 °C, Grothe (Ref. 11) used a quartz reaction vessel. On the other hand, Fisher and Simon (Ref. 2) reported that when an $AlCl_3$-NaCl melt with the $NaAlCl_4$ composition was electrolyzed in quartz crucibles, corrosion of the crucibles occurred. They concluded that this was due to Al, or low valency Al compounds dissolved in the melt. The species of Si dissolved in the melt was not identified.

Preparation and Purification of $AlCl_3$-KCl-NaCl Melts

All experimental work was carried out in the argon atmosphere of a "Lab Con Co." purge type glove box. Analyzed argon with a water content of less than 1.5 ppm was used. "Baker Analyzed" NaCl and KCl were employed, but $AlCl_3$ from a number of different suppliers was tried.

Our first experiments were conducted with the composition of the ternary eutectic containing 66 mol % $AlCl_3$, 14 mol % KCl, and 20 mol % NaCl. "Baker Analyzed" anhydrous $AlCl_3$ was used (this was certified as being 99% pure). The salts were weighed out in correct portions, well mixed, and fused on a hot plate. A greyish-brown melt was readily formed.

Other investigators (Ref. 21) have also observed this coloration and attribute it to carbonaceous material and the presence of $FeCl_3$ impurity in the $AlCl_3$. Filtration of the molten eutectic through a fine (25-μ) glass frit did not appear to change the color at all, but did remove some particulate matter.

Cyclic scans at a Pt wire microelectrode were run in order to observe the background current and obtain an indication of the nature of the impurities. The cyclic scans were recorded in the usual manner. A triangular waveform from a function generator (Exact Electronics, Inc. type 255) was fed into the input of a Wenking potentiostat (type 61RS). The potentiostatic current-voltage curves were recorded on an X-Y recorder (Houston Omnigraphic model HR-98T). Galvanostatic polarization curves were obtained by supplying a constant current from a power supply and recording the overpotential on either an oscilloscope or on the X-Y recorder.

It has been established (Refs. 22 and 23) that an Al electrode is a stable reference in this ternary eutectic, and all potentials are referred to this electrode. The actual reference electrode consisted of a coil of pure Al wire contained in a fritted compartment to prevent concentration changes from taking place in the vicinity of the electrode. A similar coil of Al wire served as counter electrode. The Pt needle electrode was made in the usual way by sealing Pt into glass.

A typical current-voltage scan is shown in Fig. 3. The anodic decomposition limit was approximately +2 V versus Al and corresponds to Cl_2 evolution. The reduction wave at +1 V versus Al was suspected to be due to the reduction of ferric ions. The addition of Al powder resulted in a marked reduction of the background current, probably by the reaction

$$Al + Fe^{3+} \rightarrow Fe + Al^{3+}$$

For subsequent measurements, $AlCl_3$ was obtained from Fluka Chemicals (Switzerland). It was stated to be anhydrous and iron-free. A ternary mixture made up with this material melts readily on a hot plate and forms a clear melt except for a darkish yellow coloration. A cyclic scan obtained in this melt is shown in Fig. 4. It appears that $FeCl_3$ is still present as an impurity. The deliberate addition of a small amount of $FeCl_3$ resulted in the current-voltage curve shown in Fig. 5.

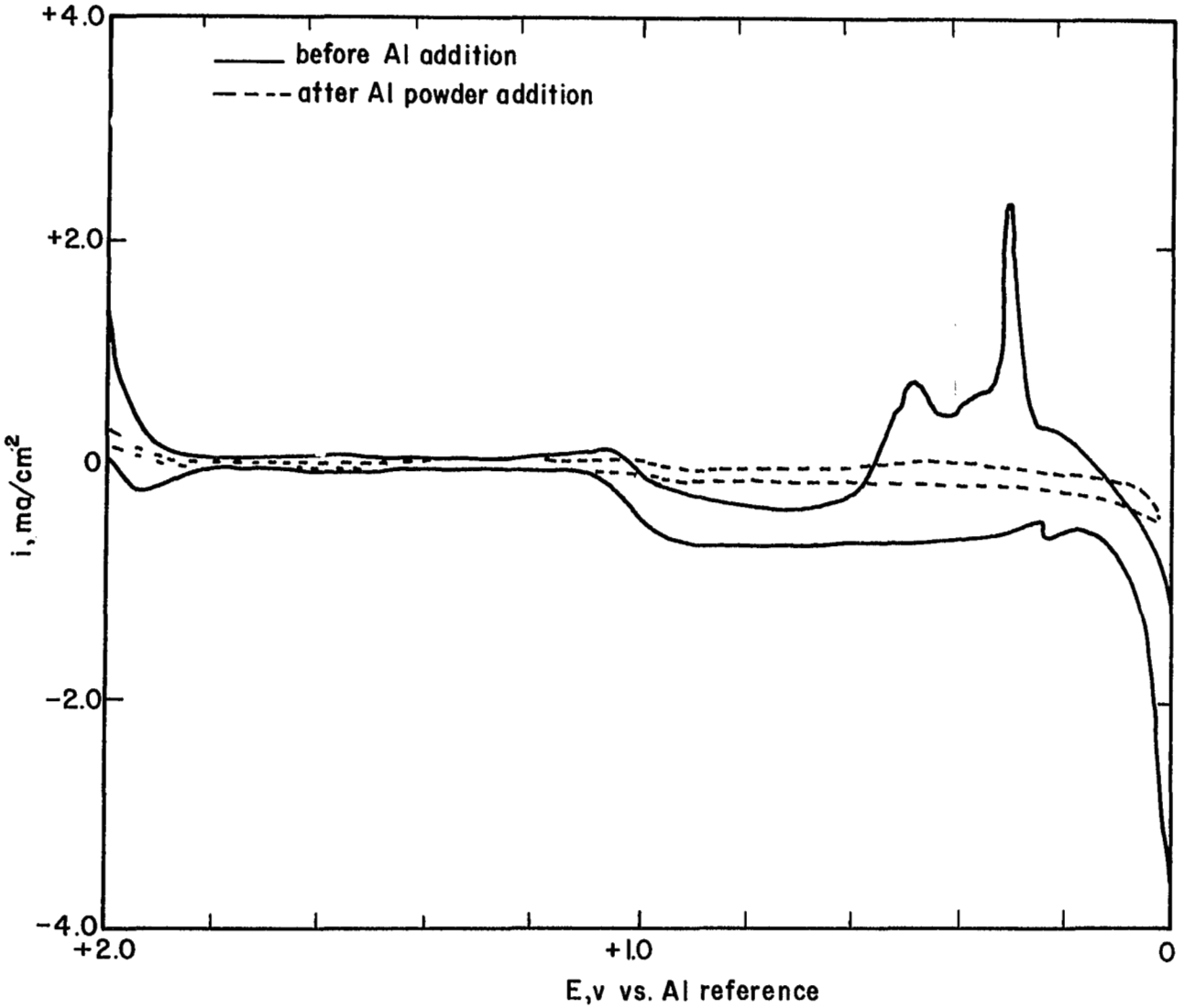

Fig. 3. Background i-V scan at Pt in eutectic melt (made with "Baker Analyzed" $AlCl_3$, 99% anhydrous; scan rate = mV/sec)

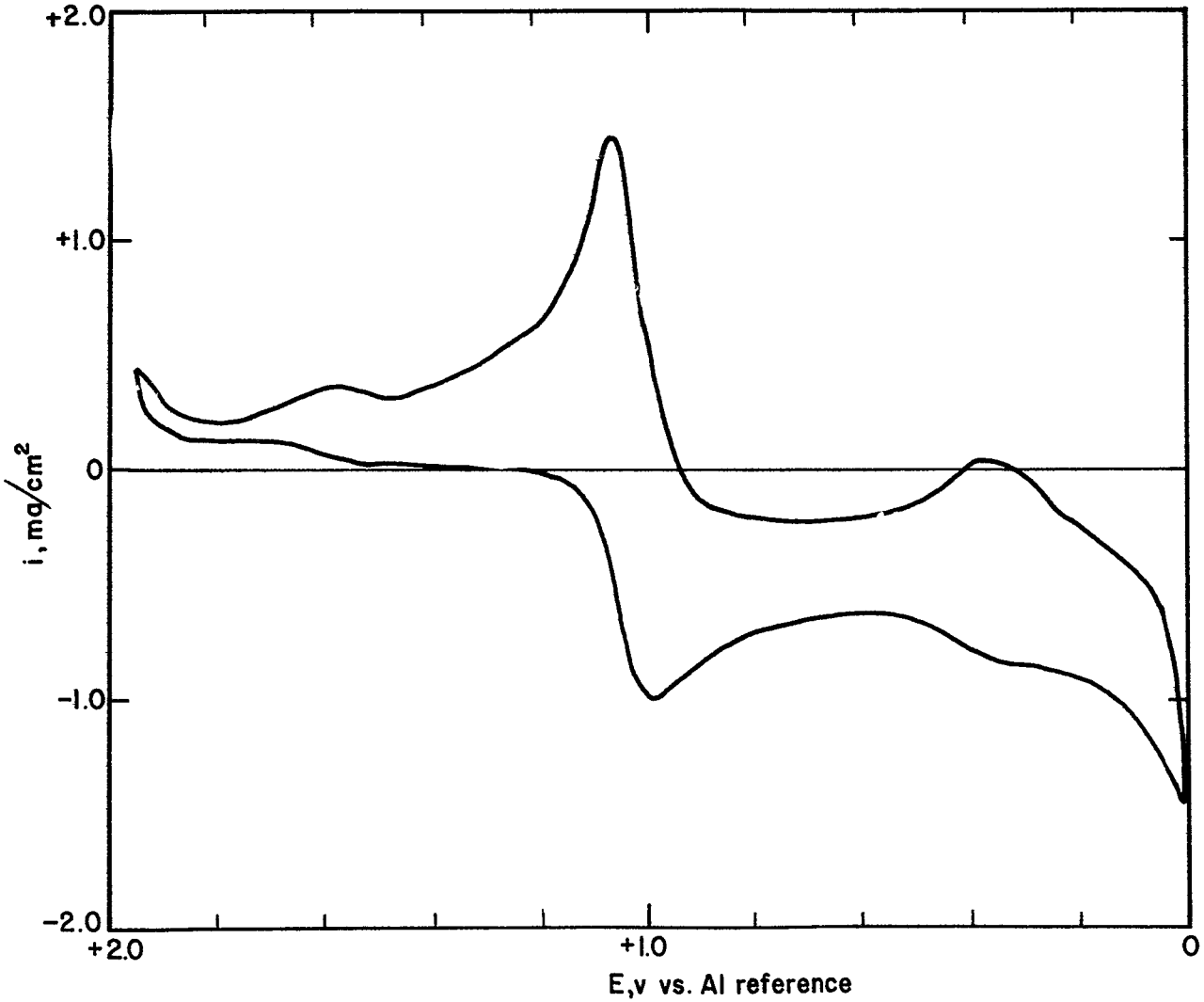

Fig. 4. Background i-V scan at Pt in eutectic melt (made with Fluka $AlCl_3$, anyhydrous and iron-free; scan rate = 160 mV/sec)

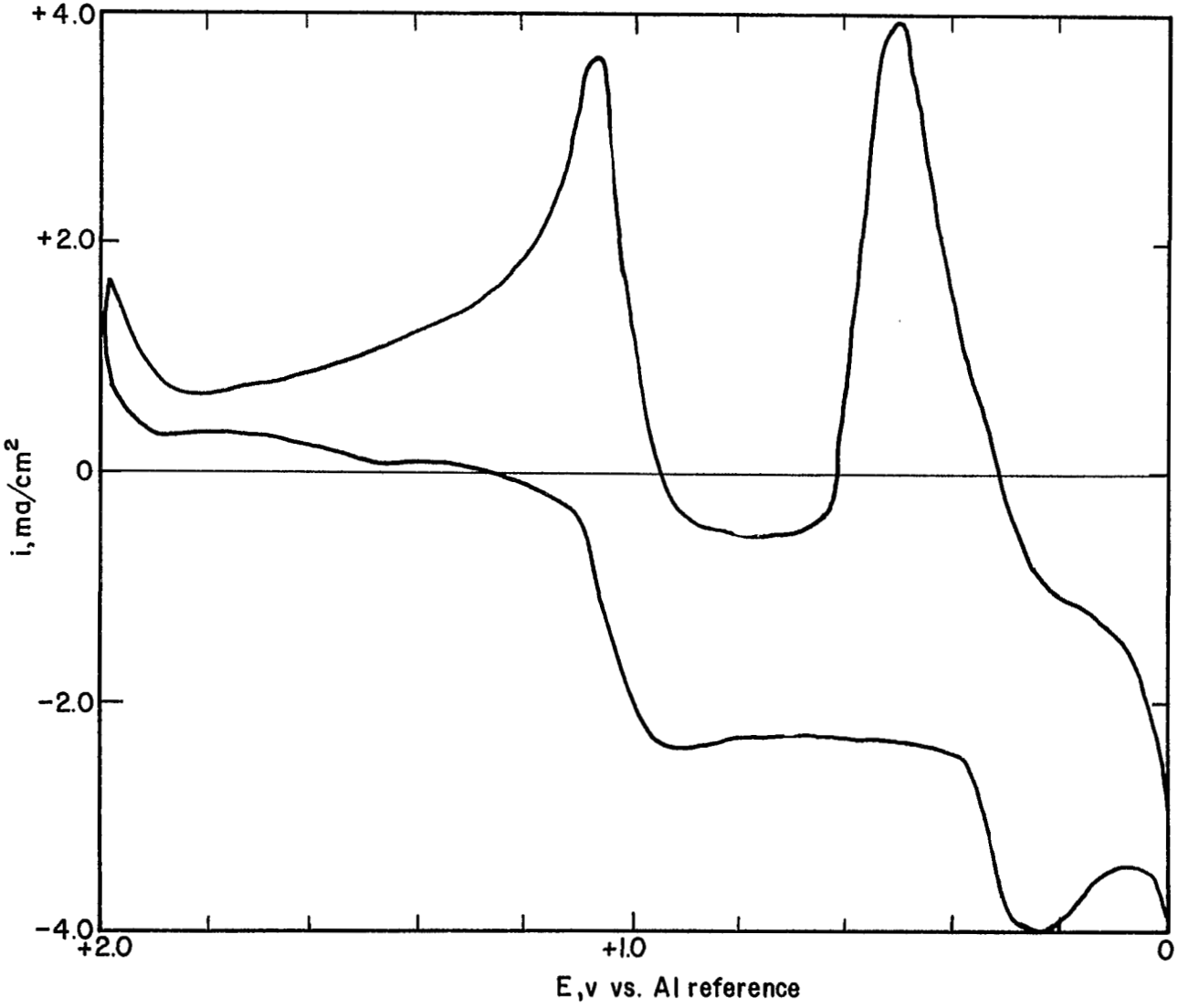

Fig. 5. Effect of small addition of $FeCl_3$ to eutectic melt made with Fluka $AlCl_3$ (scan rate = 160 mV/sec)

The curves of both Figs. 4 and 5 were obtained on Pt electrodes starting at a potential of 1.1 V versus Al. From this starting point, the potential was linearly decreased to zero, then increased linearly to 2 V, and then decreased again without a waiting time to 1.1 V. The qualitative shape of the curve is the same in both cases. The following characteristics were noted:

1 A more or less pronounced cathodic current peak was observed at about 1 V, probably due to reduction of Fe^{3+} incorporated in some layer close to the electrode. (This layer can be an adsorption layer or a still undeveloped diffusion layer.)

2. Cathodic limiting current at more negative potentials appears to correspond to the steady state reduction of Fe^{3+} to Fe^{2+}

3. A cathodic peak at about 200 mV seems to correspond to the reduction of Fe^{3+} (and Fe^{2+}) to Fe.

4. An anodic peak at about 500 mV apparently corresponds to oxidation of Fe to Fe^{2+} The current drop after the peak can be attributed to depletion of Fe or, more probably, to some passivation

5. After this passivation, a relative cathodic current is observed that can be attributed to reduction of Fe^{3+}

6. Finally, the anodic peak at 1.1 V can be interpreted as being due to oxidation of the passive film (Fe^{2+} - salt?) formed at 500 mV and of the underlying Fe. Any dissolved Fe^{2+} is oxidized to Fe^{3+} at potentials higher than 1.2 V.

From the comparison of Figs. 4 and 5 it seems reasonable to identify the major impurity present in $AlCl_3$ as Fe.

The change of coloration may be due to several factors, e.g., (1) the formation of colloidal hydroxides of heavy metals as the melt adsorbs water, (2) a higher degree of oxidation of these impurities, or (3) decomposition of organic material. Thus, in order to obtain satisfactorily clean eutectics, we have studied first the behavior of a large number of electrolytes prepared

with several $AlCl_3$ samples obtained from different manufacturers: Mallinckrodt lot RTY and TJB; Fisher lot 780679; MCB lot 25; Baker and Adamson lot B128; J. T. Baker lot 33025 and 33824; BDH (Gallard-Schlesinger, N. Y.) lot 0564110; Fluka (Buchs, Switzerland) lot 461085; Koch-Light Labs (Colnbrook, Buckinghamshire, England)

In all cased at 120 °C, the eutectic showed the brownish discoloration, which was lightest in the case of the Fluka material. Therefore, it was decided to use this material when attempting to develop a standard purification technique.

Partial success in the purification of this material has been seen in previous work after treatment of the final eutectic with aluminum turnings. The success is not complete, since the effectiveness of this treatment varied from case to case. Assuming that an aluminum oxide layer is responsible for the lack of consistency in the degree of purification, we attempted to solve this problem by using an amalgamated aluminum plate which was kept under stirring in the eutectic for 6 hr. This treatment succeeded in removing the coloration and in substantially decreasing the iron peaks of the cyclic voltammetric curves. However, a small peak at a potential of about 1.5 V was introduced which can be attributed to the presence of Hg^{2+} in solution.

Pre-electrolysis of the eutectic at 120 °C for 24 hr using Ultra Carbon U-5 grade carbon electrodes was successful in decreasing the iron peaks, but did not improve the coloration sufficiently.

After these preliminary purification attempts, the following procedure was found to yield satisfactory results. $AlCl_3$ (Fluka) was mixed with NaCl and KCl in the ratio of about 1.0 mol KCl, 1.5 mol NaCl, and 9.8 mol $AlCl_3$, giving a liquid at ~ 130 °C with a high $AlCl_3$ vapor pressure. This liquid was treated with magnesium turnings to ensure the precipitation of such impurities as iron chloride which show an appreciable vapor pressure. From this melt, aluminum chloride was evaporated at a constant temperature of 215 °C and condensed as large crystals in the cold part of the apparatus. By using two 1-ℓ resin reaction kettles as shown in Fig. 6, about 70 g of pure $AlCl_3$ can be obtained overnight. Fig. 7 shows the crystallized

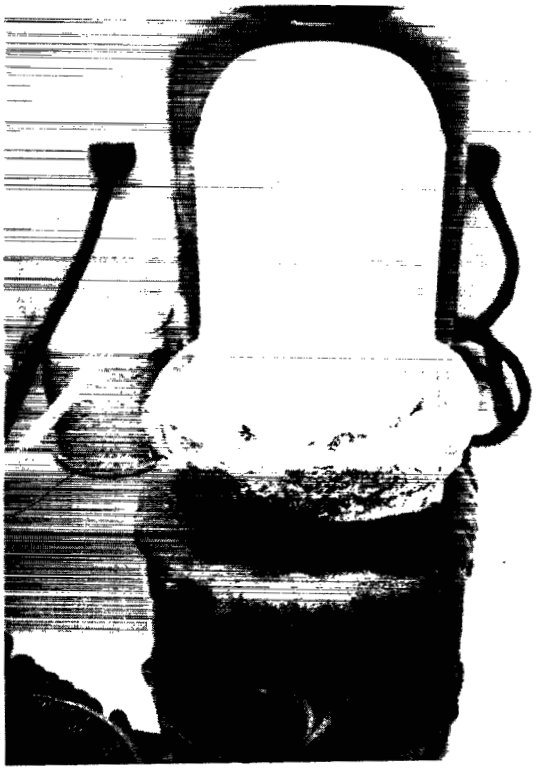

Fig. 6. $AlCl_3$ purification unit (in inert atmosphere chamber)

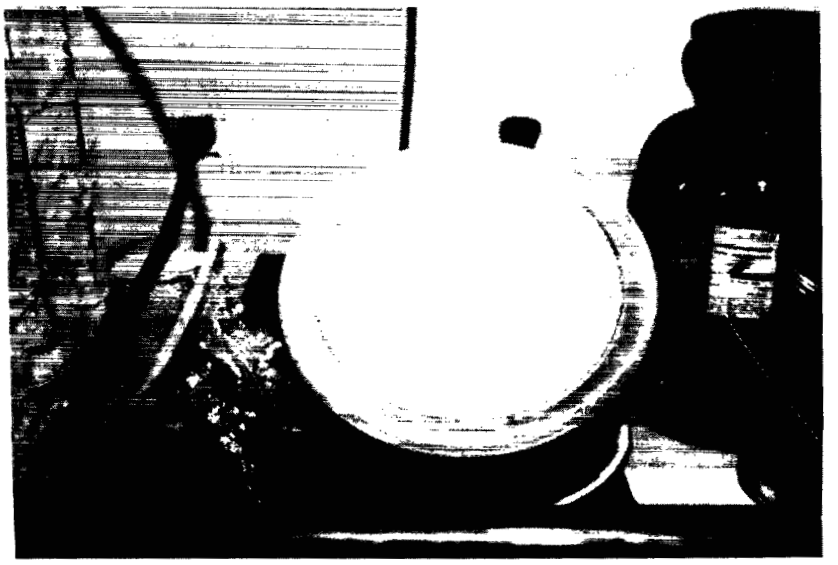

Fig. 7. View of condensed $AlCl_3$ crystals in cold part of purification unit

material in the upper (cold) part of the apparatus. The material seems to be clean as evidenced by its clearness, the production of virtually transparent eutectics, and the lack of any residual curren' in the cyclic voltammetric curves obtained with the above eutectics.

To determine qualitatively the effect of moisture, humidified argon was bubbled through the melt for a short period. It was observed that clouds of HCl gas were formed and a thin white deposit was left on the upper parts of the cell. No precipitate could be observed to form in the electrolyte. According to Letisse and Tremillon (Ref. 24) the reaction between H_2O and the equimolar NaCl-$AlCl_3$ melt is as· follows

$$2\ AlCl_4^- + H_2O \rightarrow 2\ HCl + Al_2OCl_5^- + Cl^-$$

It is presumed that a similar, if not identical, reaction occurs in the ternary eutectic.

THE CHLORINE ELECTRODE

Experimental Cell

The cell was a small (100-cc capacity) four-neck flask. The size was chosen in order to use small amounts of highly purified eutectic. The cell was operated in a hot air oven, and temperature control was ±1 °C at 120 °C. The oven was modified to allow for electrical connections to the various electrodes and to provide for Ar and Cl_2 gas inlets and outlets (see Fig. 8 for a photograph of the cell arrangement).

Stability of Carbon Electrodes

Preliminary investigations using graphite (Speer Carbon Products grade 37-G electrographite) revealed that the electrolyte wets the porous graphite quite readily, and in a short period of time considerable swelling of the electrode was noticed (see Fig. 9). Upon removing the electrode from the melt, it was apparent that the graphite had lost its structural integrity. This behavior is in contrast to tnat observed by Swinkels (Ref. 25) where the same graphite electrode was not wet by molten LiCl at 650 °C.

Disintegration of the graphite seems to be a consequence of interplanar reactions with the formation of intercalation compounds. The attack is even more pronounced in the presence of chlorine. Therefore, the compatibility of carbon electrodes from different sources and of different degrees of graphitization and porosity with respect to aluminum chloride eutectics was studied, both in the presence and the absence of chlorine. For these experiments, an $AlCl_3$-NaCl-KCl eutectic (66, 20, and 14 mol %, respectively) at 120 °C was used. When investigating the effect of chlorine, the carbon electrode was partially immersed in the electrolyte and chlorine was passed through the gas phase of the all-glass cell. The results of these experiments are presented in Table II.

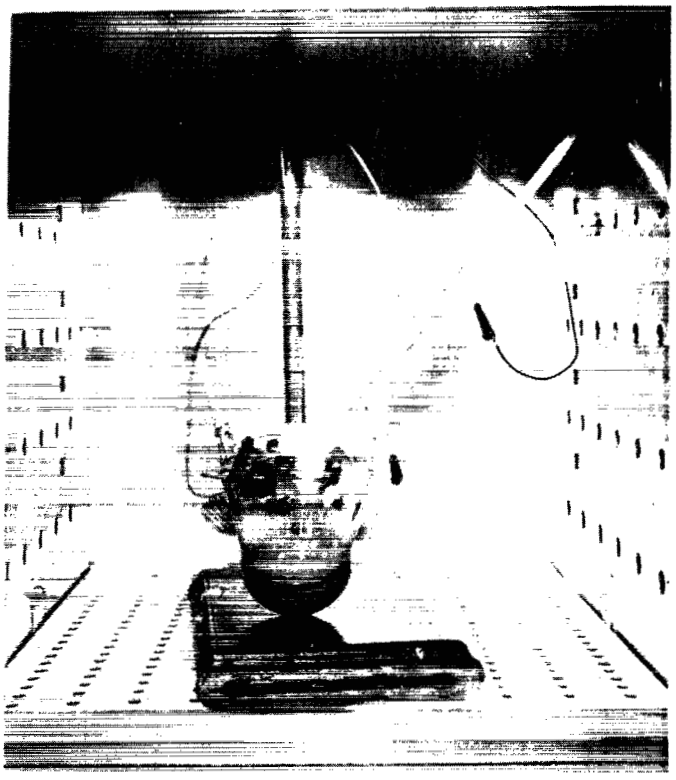

Fig. 8. Photograph of experimental cell in oven

Fig. 9. Photograph of graphite electrode after immersion in melt for 2 hr (graphite = grade 37-6, Speer Carbon Products; density = 1.35 g/cc; total porosity = 0.273 cc/g)

TABLE II
STABILITY OF CARBON-GRAPHITE MATERIALS IN $AlCl_3$-NaCl-KCl EUTECTIC IN THE ABSENCE AND PRESENCE OF CHLORINE

Material Identification	Source	Conditions: $AlCl_3$ Eutectic at 120 °C	Conditions: Cl_2 Passed Over Melt	Remarks on Cl_2 Effect
No. 37 porous carbon	Speer carbon	No attack	No attack	In contact over 48 hr
P-6038-C carbon-graphite	Pure carbon	↓	Failed	Failed in less than 15 min
PO2 dense carbon	Pure carbon	↓	No attack	
103G dense carbon	Speer carbon	↓	Failed	Failed in less than 10 min
104 dense graphite	↓	↓	↓	Failed in less than 10 min
108 dense carbon-graphite	↓	↓	↓	Failed in less than 10 min
37G porous graphite	↓	↓	↓	Failed in less than 30 min
Graphite "A"	Carborundum	Failed	↓	Rapid failure
L-50 porous carbon-graphite	Pure carbon	No attack	↓	Failure in 10 to 15 min
L-56 porous carbon-graphite	↓	↓	↓	↓
PO3 porous carbon-graphite	↓	↓	↓	↓
P3W porous carbon-graphite	↓	↓	↓	↓
CS grade dense graphite	National carbon	↓	↓	Failed in less than 30 min
Vitreous carbon	Atomergic-chemetals	↓	No attack	No attack after more than 72 hr contact with $AlCl_3$
Pyrolytic graphite	Ultra carbon	↓	↓	Pyrolytic graphite coating (a piece of plain graphite) appears to have resistance to attack

This table shows that deterioration, as evidenced by the swelling or erosion of the surface, is much more evident in the presence of chlorine. Only in the case of a few graphite samples did substantial swelling occur in the absence of chlorine. Furthermore, corrosion by Cl_2 is very much more pronounced in samples with some graphite content than in carbon samples without graphite. The samples which resisted corrosion are a Pure Carbon PO2 sample which is a high density carbon and a Speer carbon sample (no. 37) which is a porous carbon with little graphite content. Vitreous carbon from Atomergic Chemetals did not show any deterioration, even after observation of the interface under the microscope. It also seems possible that pyrolytic graphite may show sufficient compatibility with the $Cl_2/AlCl_3$-eutectic environment. As a consequence of this work, we used the no. 37 Speer carbon material to determine the feasibility of a carbon based chlorine diffusion electrode and Pure Carbon PO2 as construction material when a high density impermeable carbon was required. Vitreous carbon is suitable for kinetic studies of the chlorine reduction on smooth carbon surfaces; some preliminary results are described in the following section.

Reduction of Chlorine on Smooth Vitreous Carbon Electrodes

We investigated the intrinsic activity of pure vitreous carbon for chlorine reduction in the $AlCl_3$-KCl-NaCl (66-14-20 mol %) eutectic melt with partially immersed smooth electrodes. The meniscus is representative of the three-phase boundary of a porous gas diffusion electrode (Ref. 26). For these experiments, a rod of vitreous carbon of 0.3 cm diameter from Atomergic Chemetals Corporation was used. This carbon has a highly disordered structure which, coupled with a very high density, makes it very resistant to attack by chlorine in $AlCl_3$ eutectics. Another interesting feature of this material is its expansion coefficient which allows us to make very good seals to borosilicate glass. The electrolyte was the $AlCl_3$-NaCl-KCl eutectic which was used (unless otherwise stated) at a temperature of 120 °C. Aluminum was used as both

reference and counter electrodes. The electrolyte was saturated with argon and the chlorine gas was passed above the electrolyte level.

In an experiment with a half immersed electrode 2 cm long, an open circuit potential of 2. 1 V versus Al electrode was obtained. Starting from this potential, the potentiostatic current-potential curve of Fig. 10 was obtained in which each point was measured after waiting 5 min. To demonstrate that the current was produced by chlorine reduction on carbon, chlorine was replaced by argon and the decay of current at constant potential recorded as a function of time (Fig. 11). After renewed introduction of chlorine, the current increased again to a value close to the previous value. The delay in reaction to gas changes can easily be explained by the gas volume in the electrochemical cell and tubings. The effect of potential on current was further investigated, as shown in Fig. 12, by following the current as a function of time at constant potential.

Fig. 13 shows that while the currents are rather stable at the low polarizations, larger fluctuations occur at increasing polarizations. These are probably due to the effect of the increasing depth of penetration of the Cl_2 reduction along the thin film with increasing polarization, and the resulting sensitivity of the results to convection and to drying of the film.

In general, the results reported here can be considered only as semiquantitive, since the film is not well defined due to the above mentioned changes caused by convection or drying of the film. However, these results can be interpreted as clear proof that pure carbon is intrinsically active in catalyzing the reduction of Cl_2 in $AlCl_3$-NaCl-KCl electrolytes.

A series of tests were carried out to determine the contribution of the immersed part of the electrode in producing the current in an experiment in which the stagnant electrolyte had been saturated with chlorine. This experiment did show that there was no decrease in current when the immersed part of the electrode was reduced practically to zero. Another series of experiments performed to establish approximately the effective

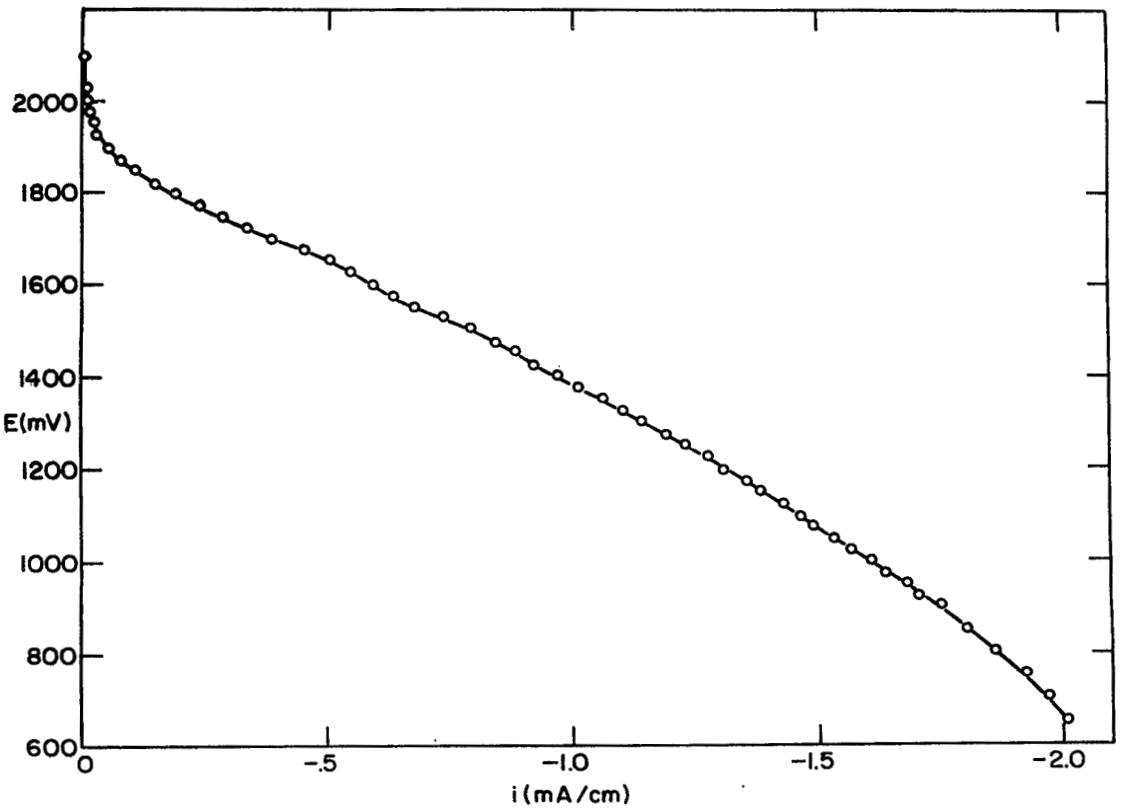

Fig. 10. Potentiostatic current-potential curve for Cl_2 reduction on partially immersed vitreous carbon electrode

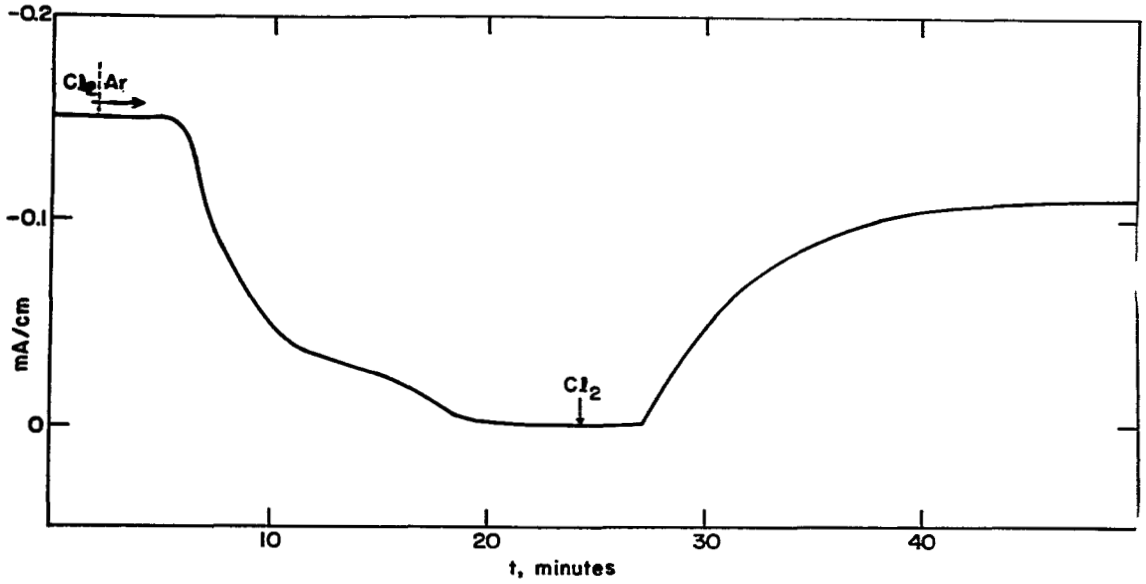

Fig. 11. Effect of Cl_2 gas on current obtained with partially immersed vitreous carbon electrode (potentiostated at 1.8 V versus Al reference electrode)

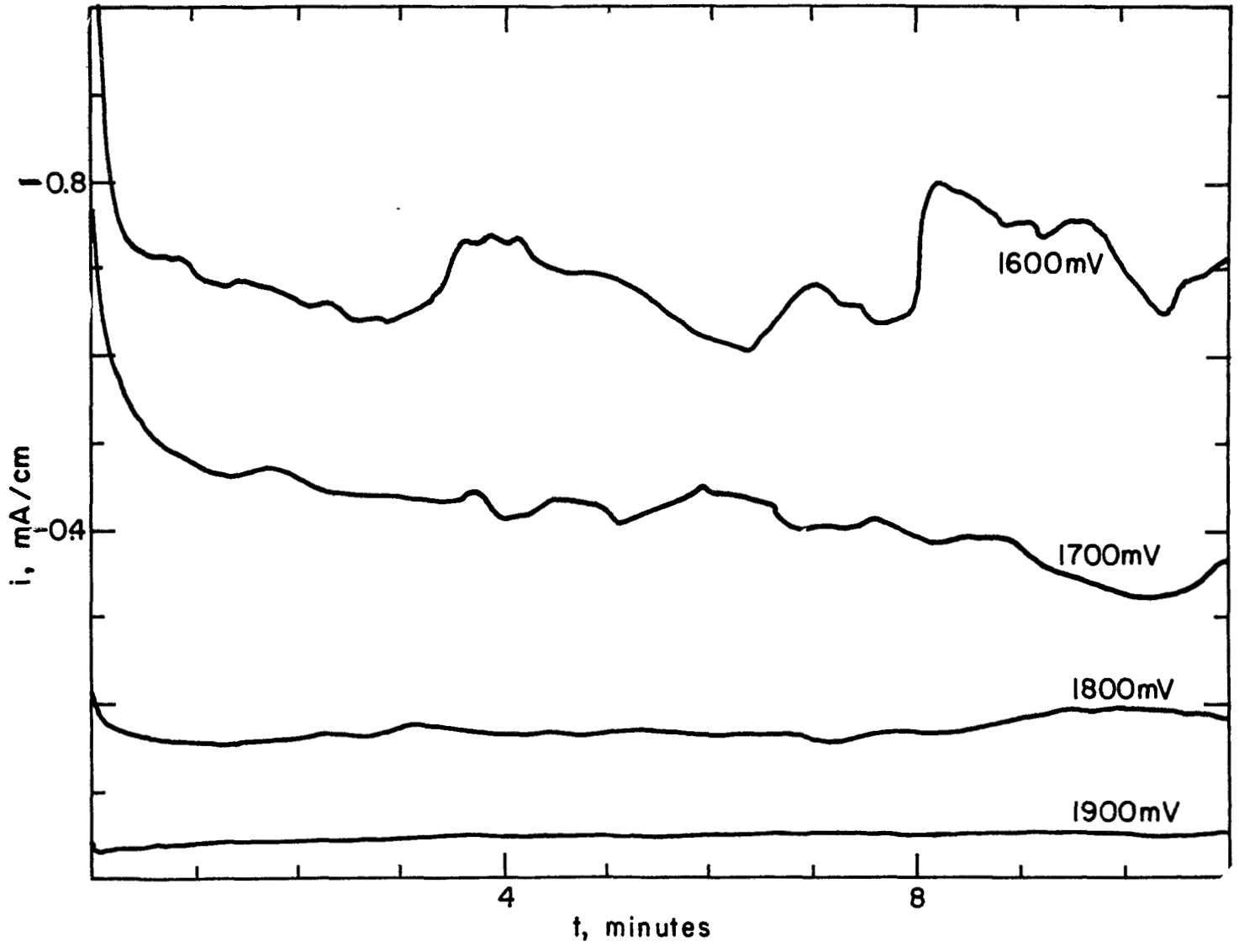

Fig. 12. Effect of potential on potentiostatic current-time curves for Cl_2 reduction on partially immersed vitreous carbon electrode

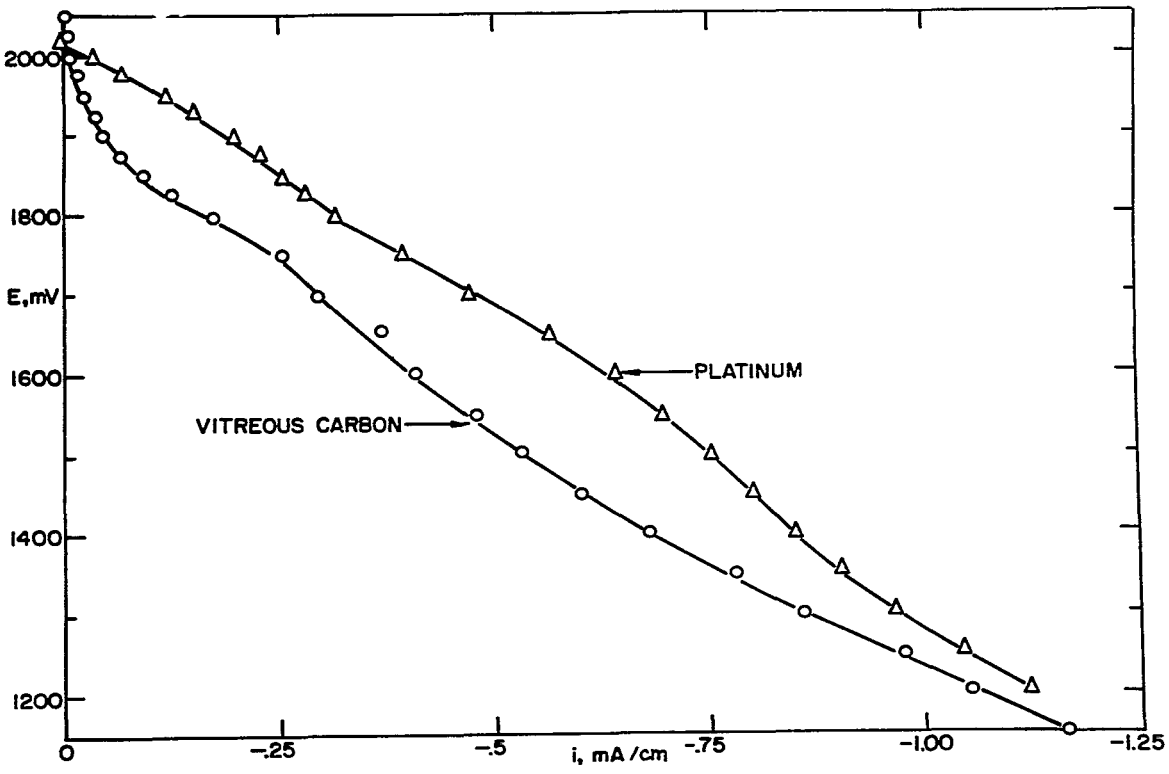

Fig. 13. Comparison of i-E curves for Cl_2 reduction on partially immersed platinum and vitreous carbon electrode

length of the meniscus (and thin film) showed that reduction of the immersed part of the electrode down to 0. 2 cm did not substantially affect the magnitude of the current.

In order to ascertain the effect of electrode pretreatment, the electrode was anodically polarized for 0. 2 min to evolve chlorine at a current density of +0. 5 mA. After this pretreatment, the activity for chlorine reduction of the carbon as a partially immersed electrode was substantially unchanged. The same was true after cathodically polarizing the electrode for 0. 1 min at 1000 mV potential.

In another experiment, the flow of chlorine was greatly increased above the electrolyte surface; this resulted in an increase of the current which could be attributed to either a drying of the film or to an increase of the chlorine partial pressure at the interface with the film. This experiment showed that in order to use this type of data for quantitative measurements, extreme care should be taken in controlling the gas phase concentration with respect to chlorine and $AlCl_3$ vapor.

To compare the activity of carbon with that of platinum, two experiments were carried out in the same melt and under the same conditions, first using a carbon electrode and then a platinum electrode with the same degree of immersion. The results, given in Fig. 13, show an overall higher activity of platinum versus that of carbon. The fact that the open circuit of the platinum electrode is about 60 mV lower than that of the carbon electrode can be construed as an indication of corrosion of the platinum electrode at the theoretical potential of the chlorine electrode.

Conclusions

The work with partially immersed vitreous carbon electrodes indicates that carbon has enough intrinsic activity to warrant the testing of an unactiviated porous carbon electrode as chlorine cathode in the $AlCl_3$-NaCl-KCl eutectic. In addition, the experience with vitreous carbon electrodes shows that this material should be ideally suited for studying

the reduction kinetics of the dissolved chlorine using a rotating disk and a stationary electrode in pure $AlCl_3$ eutectics. Finally, the study of compatibility of carbon materials for chlorine electrodes in $AlCl_3$ eutectics has uncovered carbon samples which appear suited for the construction of chlorine cathodes for operation in this electrolyte.

THE ALUMINUM ELECTRODE

Experimental

An electrochemical cell was built using two O-ring joings with 50-mm inside diameter. An overall picture of the cell arrangement is given in Fig. 14.

The cell top contained four tubes and a Teflon needle valve for the gas inlet and outlet and for the connections to the electrodes. A Viton O-ring was used as gasket. The electrodes and the gas inlet tube were connected with Teflon Swagelok fittings, using stainless steel back ferrules. The aluminum working electrode consisted of a pure aluminum wire 1.2 cm in length and 1 mm in diameter. The rest of the aluminum wire was covered with several layers of shrinkable Teflon. The reference electrode was also aluminum contained in a separate compartment with a narrow opening to protect it from changes in electrolyte concentration. An aluminum wire wound in a spiral along the inside of the vessel served as counter electrode. The cell also contained a platinum electrode sealed into glass for measurements of the electrolyte background.

The gas inlet part of the cell was connected to a tank of argon over a pressure control consisting of an electromagnetic valve and a mercury contact manometer. Thus, we could keep a constant adjustable argon pressure (normally, a positive pressure of 10 to 20 torr was used). This arrangement also indicates immediately if there is a leakage in any of the cell joints.

For the experiments, the cell was filled and assembled tightly in the glove box, then transferred to the oven and connected to the argon line. The measurements were made without gas passing through the cell to avoid concentration changes resulting from the appreciable vapor pressure of $AlCl_3$ over the melt.

The appearance of the melt was clear, but it turned grayish with time. There seemed to be a slight interaction between the melt and Teflon resulting in a dark discoloration of the Teflon at the interface.

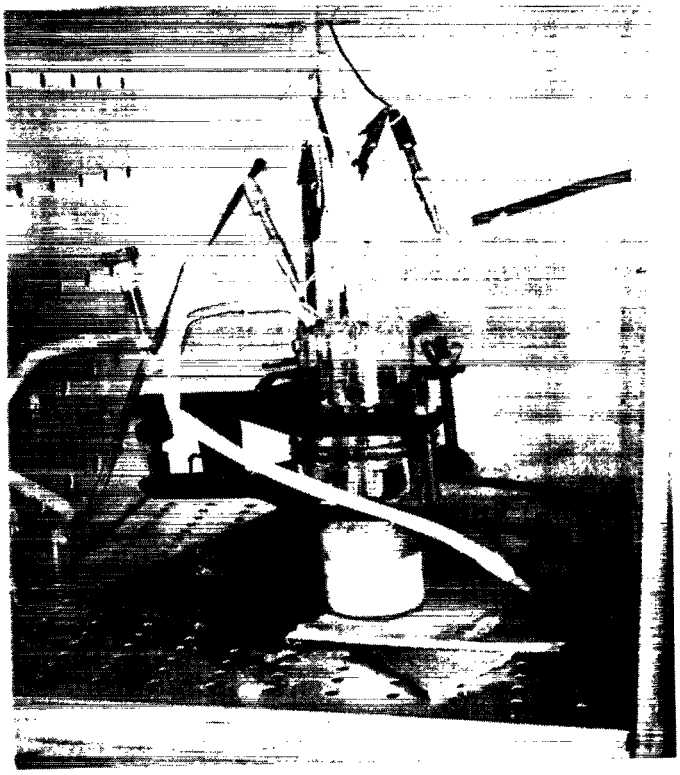

Fig. 14. Electrochemical cell

Results and Discussion

The experiments were conducted at two different temperatures: 157 and 105 °C, and with two different melt compositions: melt I of $AlCl_3$-KCl-NaCl (67-13.6-19.4 mol %) and melt II of 59-17-24 mol %. Typical current-voltage curves in quiescent electrolytes are shown in Figs. 15 to 17, and 19 and 20.

All current-potential and current-time curves show more or less pronounced passivation phenomena. Their dependence on charge passed through the electrode, on electrolyte composition, and on temperature will be discussed in detail in the following paragraphs.

Effect of Potential and Time

Anodic behavior. -- The anodic potential sweeps in Figs. 15 to 17, 19 and 20 show that the anodic passivation of the Al electrode does not occur at a constant defined potential. A closer examination shows that it is not the potential but rather the charge (current and time) which is the parameter determining the sudden current drop. Fig. 17 shows the correlation between anodic passivation and cathodic prepolarization. Comparison of the anodic and cathodic charges (represented by the area underneath the i-t curve) shows that they are nearly equal. This is even more obvious from Fig. 18 which shows the cathodic and anodic currents versus time upon potentiostatic polarization to ±100 mV for periods of varying length. This behavior seems to indicate that melt I (which is $AlCl_3$ rich) cannot tolerate much more anodic formation of $AlCl_3$ without precipitating it as an insoluble passivating salt. On the other hand, if by cathodic pretreatment we form a diffusion layer close to the electrode which is poor in $AlCl_3$, then we are able to polarize the electrode anodically for a time necessary to replenish the initial $AlCl_3$ concentration until passivation appears. Parallel to the behavior of Fig. 18, one observes that the aluminum electrode which is shiny after cathodic polarization assumes a very dull appearance upon passivation. The fact that in Fig. 18 the anodic and cathodic charges are almost equal indicates a rather compact diffusion layer with practically no convection. As the cathodic prepolarization time is increased above the values shown in Fig. 18, the charge obtained prior to anodic passivation becomes smaller than the cathodic charge, as one would expect.

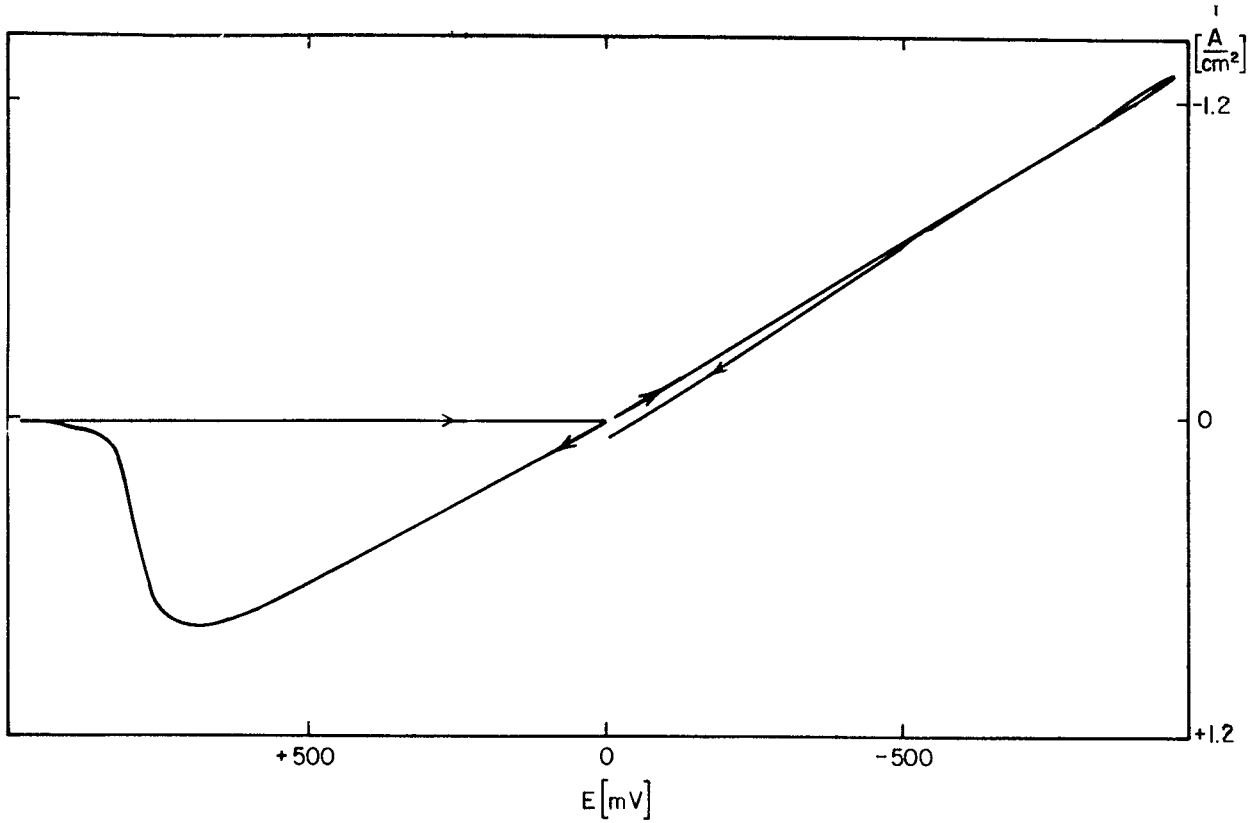

Fig. 15. Two triangular scans on Al electrode in melt I at 157 °C and 20 mV/sec (0 mV to +1 V back to 0 mV, and 0 mV to −1 V back to 0 mV; no IR correction)

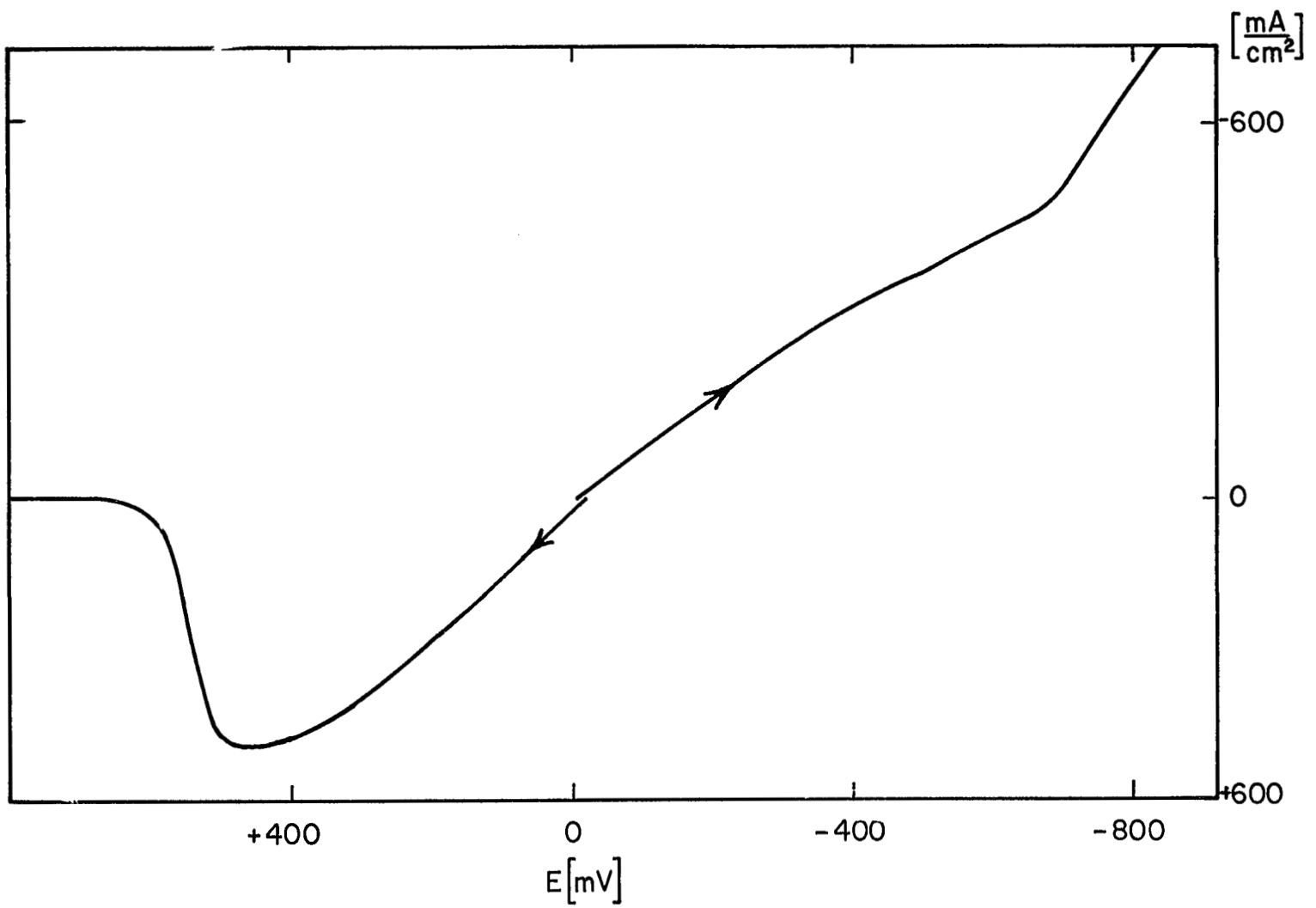

Fig. 16. Linear potential scans in anodic and cathodic directions starting from reversible potential (obtained on Al electrode in melt I at 115 °C and 400 mV/min; no IR correction)

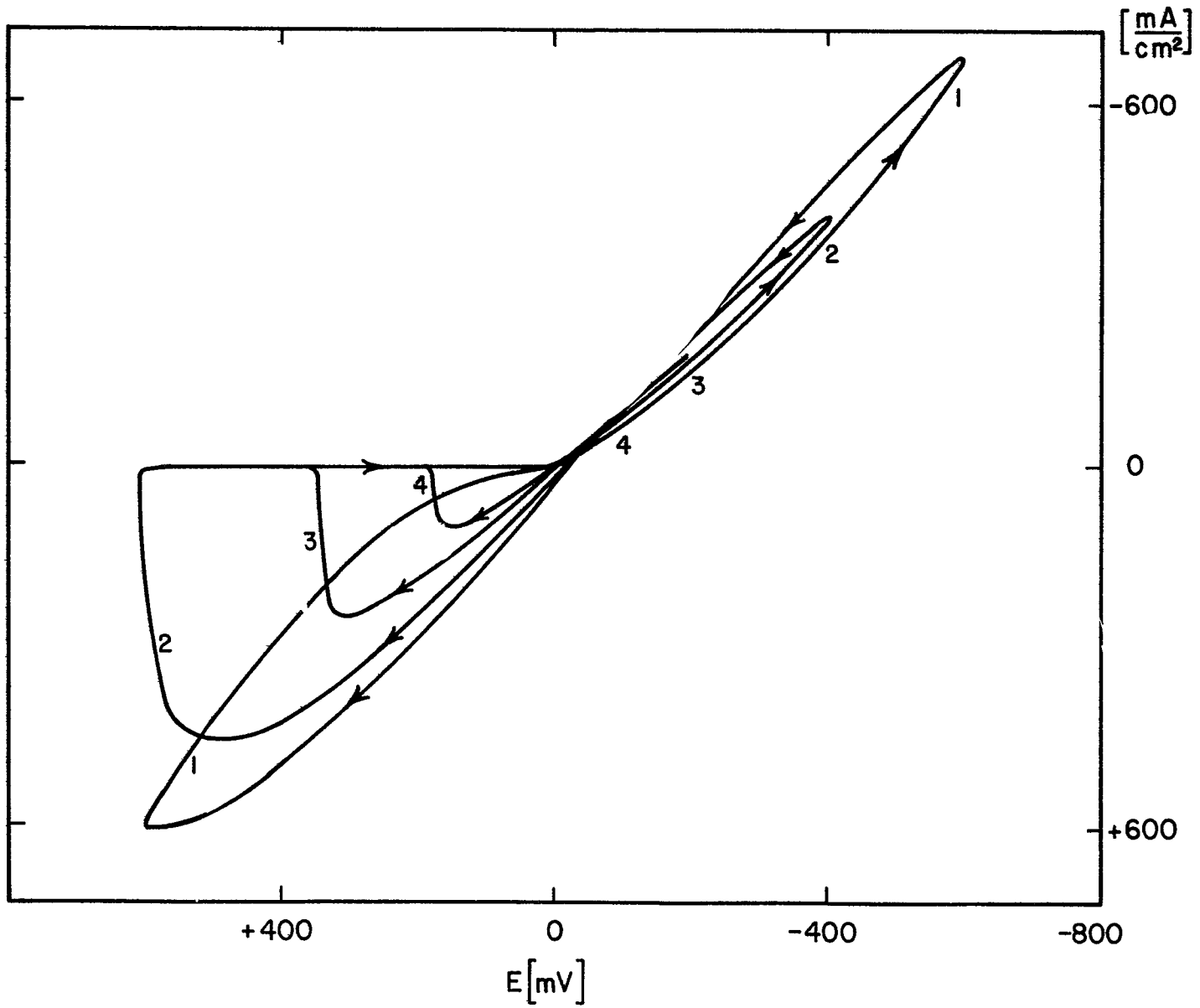

Fig. 17. Triangular potential scans on Al electrode in melt I at 105 °C and 400 mV/min (from mV to E_{cath} to E_{anod} back to 0 mV; no IR correction)

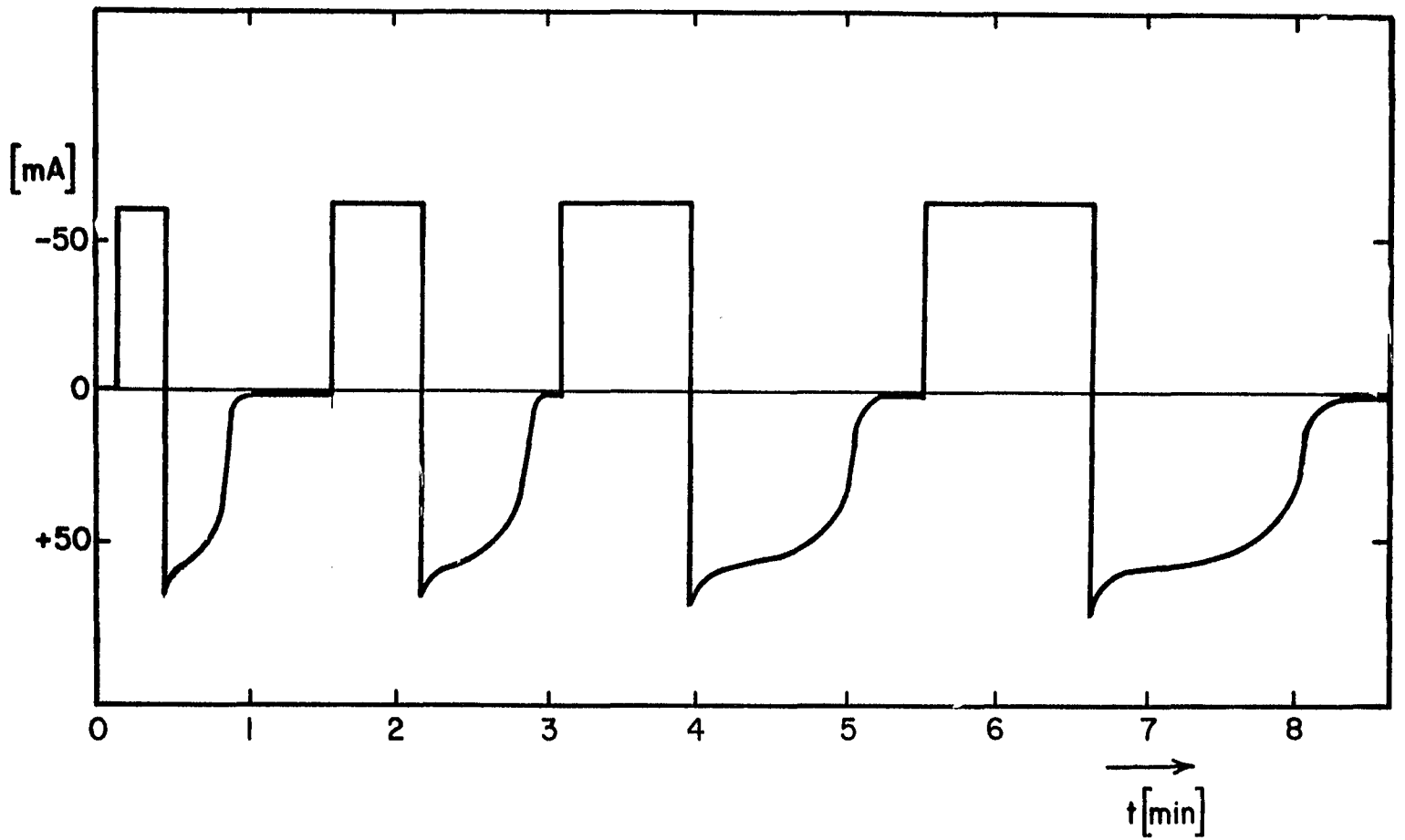

Fig. 18. Potentiostatic current-potential curves on Al electrode in melt I at 156 °C (cathodic potential pulses of −100 mV and variable length followed by anodic pulses of +100 mV; no IR correction)

1. E_{cath} = 600 mV
2. E_{cath} = 400 mV
3. E_{cath} = 200 mV
4. E_{cath} = 100 mV

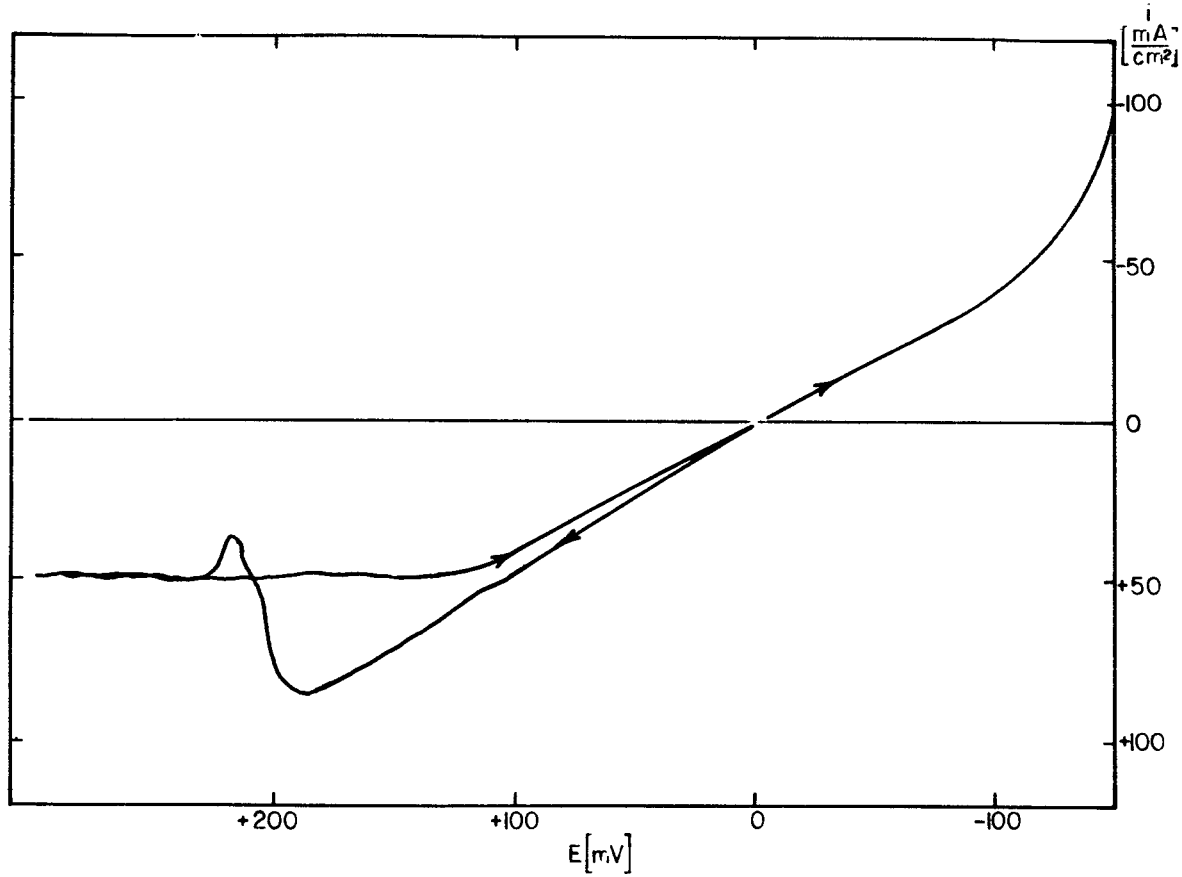

Fig. 19. Triangular anodic potential scan (0 mV to 300 mV back to 0 mV) and linear cathodic potential scan (0 mV to −150 mV) on Al electrode in melt II at 157 °C and 20 mV/min (no IR correction)

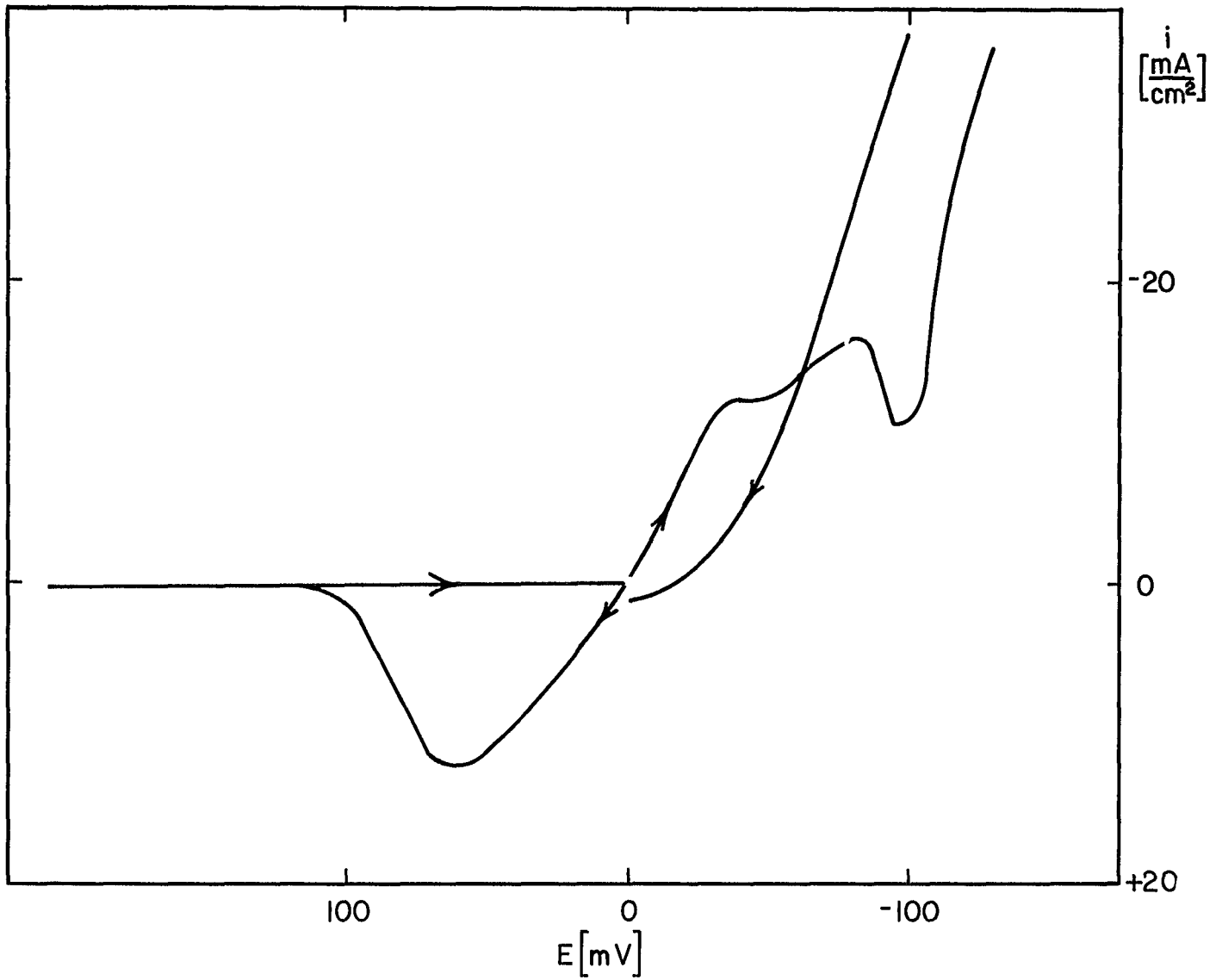

Fig. 20. Triangular cathodic potential scan (0 mV to −150 mV back to 0 mV) and anodic potential scan (0 mV to 200 mV back to 0 mV) on Al electrode in melt II at 105 °C and 20 mV/min (no IR correction)

Cathodic Behavior. -- If the above explanation holds, one should expect a similar passivation effect at cathodic currents. In fact, current voltage sweeps show indications of such a behavior (Figs. 16 and 20). In all cases, however, a subsequent current increase is found after indications of passivation. This is due to dendrite formation at the aluminum electrode. Long shiny aluminum dendrites can easily be seen growing into the electrolyte, thus enlarging the active surface area.

Dendrite growth again is not connected directly to potential but rather to current and time. There seems to be a current value below which little dendrite formation is noticeable. This limit changes with conditions. In some experiments such as those in Fig. 18, it was observed that cathodic currents at a set potential stayed constant for a certain time and then began to increase as a consequence of dendrite formation. Although more detailed information on the parameters governing dendrite formation is required, our results indicate the strong effect of concentration polarization and/or ionic conductivity on dendrite formation.

Effect of Melt Composition

Information on the effect of melt composition can be obtained by comparing Figs. 15 and 19 (obtained at 157 °C) or 16 and 20 (obtained at 105 °C). The most obvious difference between the two melts is the much higher steady state anodic current after passivation in melt II (Fig. 19). On the cathodic side, a deviation from the linear current potential behavior appears at much larger current densities in melt I than in melt II (compare Figs. 16 and 20). This again confirms our explanation of salt formation at the electrode. Melt II, which is less concentrated in $AlCl_3$, can support higher anodic current densities (that means it can accept more Al^{3+} without forming insoluble $AlCl_3$) than melt I. The latter, however, since it is more concentrated in $AlCl_3$, will be able to support higher cathodic currents before forming a passivating salt layer due to X-$AlCl_4$ precipitation (we disregard for the moment the additional complication of dendrite formation). The anodic current maximum in Fig. 19 is very likely due to supersaturation

of the melt close to the electrode. After the first crystal has formed, the supersaturation breaks down. This is responsible for the following current dip.

Thus, the limiting value of the steady state current, besides depending on the usual transport properties, also depends on the capacity of the melt to accommodate concentration changes without surpassing the solidus line of the phase diagram. The latter is clearly a function of melt composition.

Effect of Temperature

The effect of temperature on the current-voltage behavior of the aluminum electrode in the molten salt electrolyte can be seen most clearly by comparing Figs. 19 and 20 obtained using the same melt. Although a considerable steady state current can be obtained at 157 °C ($\sim$ 50 mA/cm^2), this steady state current is practically zero at 105 °C.

The temperature affects the results in several ways. First, there is the temperature dependence of the usual transport phenomena: for example, the viscosity decreases, and the diffusion coefficients increase with rising temperature. Much more important in our case, however, are considerations concerning the NaCl-KCl-$AlCl_3$ phase diagram. We mentioned earlier the key role of solid salt formation. How large a concentration change is necessary to surpass the solidus line of the phase diagram is, to a large extent, a function of temperature (besides initial melt composition). That transport phenomena are current limiting has been established also by stirring. Following this stirring, the current increased instantaneously and then exponentially approached its old value.

The temperature will surely have an effect on dendrite growth, since this is controlled by diffusion and ohmic polarization. Further changes in conductivity due to varying dissociation constants and changes in complex formation with temperature are to be expected. These problems can, however, not be discussed more closely on the basis of presently available data.

Effect of Current on Activation Polarization

The work discussed in the preceding sections has been concerned with passivation phenomena caused by concentration changes. In addition to this, no correction for ohmic polarization (caused by the resistance between working and reference electrode) has been made. It is of great interest now in order to evaluate the Al electrode for operation in a battery (and also for studies on the mechanism of this electrode) to ascertain the value of its activation polarization and the effect of current on this activation polarization. For this purpose, we have used galvanostatic pulses, both anodic and cathodic, with various current densities. A typical oscilloscope trace is shown in Fig. 21. The ohmic resistances calculated from the sudden potential jumps and the approximate activation overvoltages from all measurements are given in Tables III to VI.

From this data, one obtains the following average resistances between working and reference electrode:

	Resistance, ohms	
	105 °C	157 °C
Melt I	3.1	2.3
Melt II	2.6	1.8

As expected, the resistance decreases with increasing temperature in both melts. At a constant temperature, it increases with increasing $AlCl_3$ concentration.

A plot of activation polarization versus current density is shown in Fig. 22. For pure comparison purposes we also show a line representing the following equation:

$$i = i_0 \exp\left(\frac{\alpha z F}{RT}\eta\right)\left[1 - \exp\left(\frac{-zF}{RT}\eta\right)\right]$$

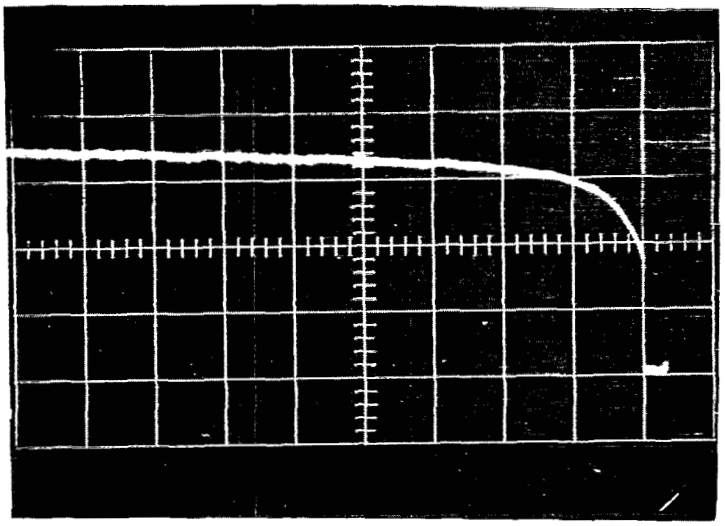

Fig. 21. Cathodic galvanostatic potential-time curve on Al electrode in melt II at 157 °C (I = 4.8 mA; ordinate scale = 5 mV/div; abscissa scale = 10 msec/div)

TABLE III
157 °C MELT I GALVANOSTATIC PULSE MEASUREMENTS

i, mA	U, mV	R, ohms	η, mV
Cathodic			
27.0	61.3	2.27	5.4
9.4	22.0	2.35	3.9
9.4	21.5	2.29	3.3
4.8	9.7	2.02	
0.6	1.3	2.15	1.7
1.9	4.7	2.48	2.7
0.6	1.5	2.51	1.8
0.6			1.9
48.0	107.5	2.24	5.4
100.0	215.0	2.15	10.7
Anodic			
0.6	1.4	2.33	1.0
1.9	4.3	2.25	1.8
9.4	21.5	2.29	4.3
48.0	107.5	2.24	4.3
100.0	223.1	2.23	6.4

TABLE IV
105 °C MELT I GALVANOSTATIC PULSE MEASUREMENTS

i, mA	U, mV	R, ohms	η, mV
Cathodic			
100.0	301.1	3.01	21.5
48.0	139.8	2.91	16.1
1.9	8.1	4.22	6.9
9.4	32.3	3.43	11.8
0.6	3.5	5.91	6.6
Anodic			
1.0	3.0	3.17	0.8
0.6	1.8	2.96	
4.8	14.5	3.02	3.2
27.0	89.2	3.31	27.9
100.0	301.1	3.01	23.6

TABLE V
157 °C MELT II GALVANOSTATIC PULSE MEASUREMENTS

i, mA	U, mV	R, ohms	η, mV
Anodic			
27	48	1.78	5.1
48	86	1.79	5.7
9.4	17.1	1.82	4.0
0.95	1.8	1.91	1.8
1.91	3.6	1.92	4.0
0.6	1.7	2.1	1.9
0.95	1.8	1.91	2.2
9.4	17.1	1.82	3.7
4.8	9.1	1.9	3.4
100	182	1.82	
Cathodic			
48	86.6	1.8	9.1
100	182	1.82	
9.4	17.1	1.82	3.4
0.95	1.7	1.8	3.4
4.8	9.0	1.88	7.4
0.6	1.1	1.8	1.7
1.91	3.2	1.67	5.7

TABLE VI
105 °C MELT II GALVANOSTATIC PULSE MEASUREMENTS
(INCREASED ELECTRODE AREA DUE TO THE PRESENCE OF DENDRITES)

i, mA	U, mV	R, ohms	η, mV	η, mV (Passive Electrode)
Anodic				
0.6	6.7	11.4		14.8
0.95	3.8	4.07	2.7	
1.91	8.0	4.16	7.4	
0.6	5.9	10		2.9
9.4	24	2.55	9.7	
0.95	10	10.5		5.1
1.91	1770	930		228
Cathodic				
1.91	5.5	2.86	3.4	
100	217	2.17		
48	120	2.5	17.1	
0.6	1.8	3.04	1.1	
0.95	2.6	2.76	1.9	

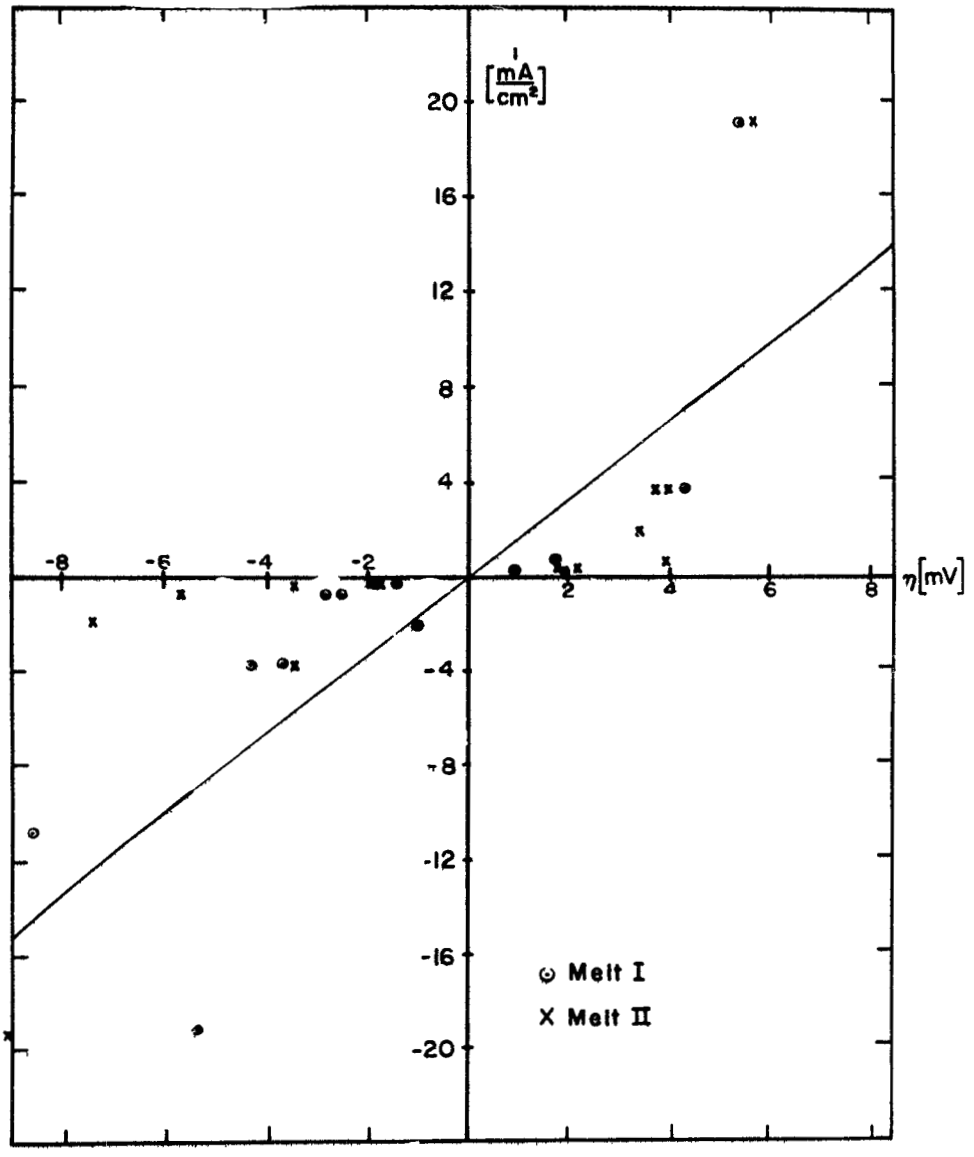

Fig. 22. Current density versus initial activation polarization for Al electrode at 157 °C

where $\alpha = 0.5$, $z = 3$, and $i_0 = 20$ mA/cm^2. It can be seen that deviations of about 5 mV in both the anodic and cathodic directions cause very little current to flow (much less than would be expected, for instance, from a pure activation controlled reaction with $i_0 = 20$ mA/cm^2), while for activation polarizations higher than 5 mV, the current becomes larger than would be expected from the above activation controlled process. This transient behavior has to be interpreted later taking into consideration that this process is an electrocrystallization process, far more complex than a purely activation controlled one.

Conclusions

The behavior discussed above in detail leads us to the following conclusions:

1. The passivation effect is due to formation of a solid salt layer at the electrode surface caused by concentration changes during current flow.

2. The occurrence of passivation is not dependent on potential, but rather on current and time, i. e., on charge passed through the electrode. It also depends on the transport properties of the melt.

3. The occurrence of salt formation depends on the compositional stability of the melt towards concentration changes. It is strongly dependent on melt composition (see phase diagram) and on temperature.

4. At cathodic currents, dendrite formation occurs at the aluminum electrode. Detailed conditions would have to be investigated.

5. The aluminum electrode itself is highly reversible and able to support large current densities at low activation overvoltage.

6. The polarization observed in the experiments is almost completely ohmic in nature. It again depends on melt composition and temperature.

FEASIBILITY TEST OF Al/Cl_2 CELL

In order to demonstrate the feasibility of an Al/Cl_2 battery with $AlCl_3$-NaCl-KCl electrolyte, a cell was built using a porous carbon electrode as the chlorine electrode, and operated in the primary mode. Fig. 23 shows the chlorine cathode arrangement. The porous electrode was made from a sample of Speer Pure Carbon no. 37 (previous work had shown this to be corrosion resistant). The material had been machined to give a cylinder 4.5 cm high and 1.9 cm in diameter, with an internal concentric hole 0.3 cm penetrating to 0.8 cm of the base of the cylinder. The cylinder was externally threaded at the open end and was screwed to an internally threaded Teflon tube. Electrical contact was made by means of a platinum wire attached to the thread.

Fig. 24 shows the cell arrangement. The aluminum electrode was a cylinder 73 cm^3: 5.3 cm high and 4.3 cm in diameter, concentric to the carbon cylinder. An Al reference electrode was placed in a glass tube external to the Al cylinder, with a Luggin capillary which was introduced through a hole in the Al electrode so that the tip of the Luggin capillary was 2 mm from the carbon electrode. The electrolyte was a mixture of $AlCl_3$, NaCl, and KCl with a composition of 66-20-14 mol %, respectively. The operating temperature was 150 °C. The chlorine electrode was operated at a pressure of about 10 psig, which allowed a slight bubbling of chlorine. This pressure had been adjusted to give the highest current density. The curve shown in Fig. 25 was obtained with this cell. This curve shows that using a noncatalyzed carbon electrode, an Al chloride cell can be built with at least 20 mA/cm^2 over 1.8 V cell potential. The cell was operated potentiostatically, but was briefly discharged through a resistor to confirm its capacity to generate power. The nature of the limiting current and methods to improve the performance of the chlorine electrode have to be the subject of further work.

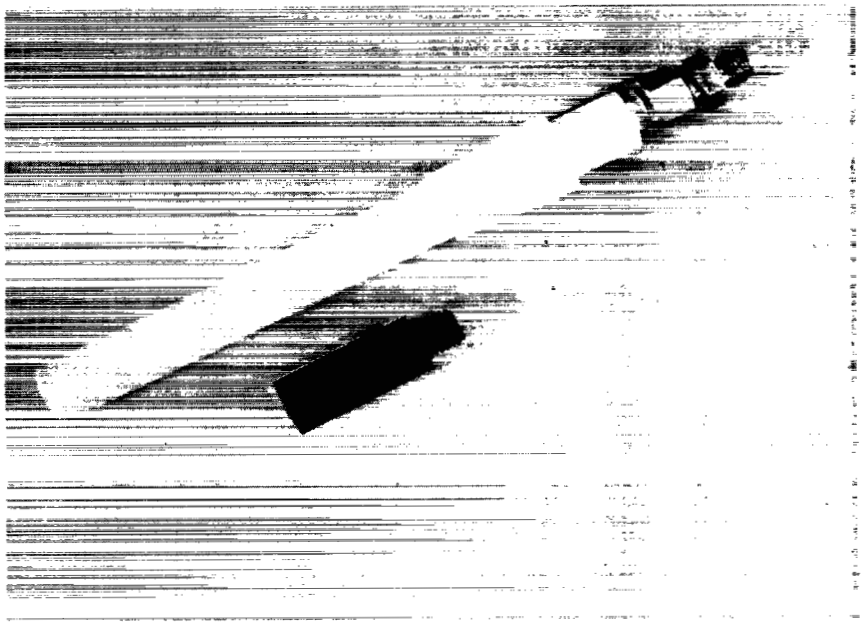

Fig. 23. Porous carbon electrode

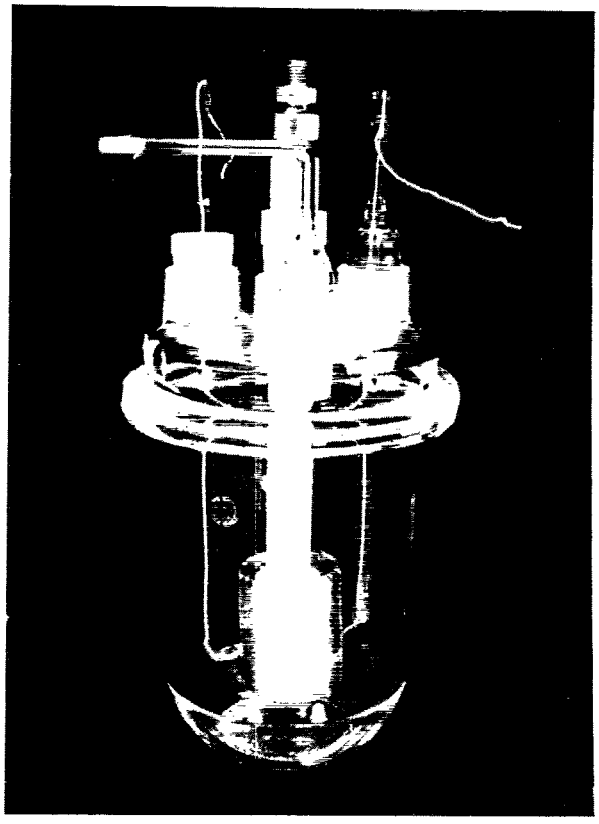

Fig. 24. Cell arrangement for feasibility test of Al-Cl battery

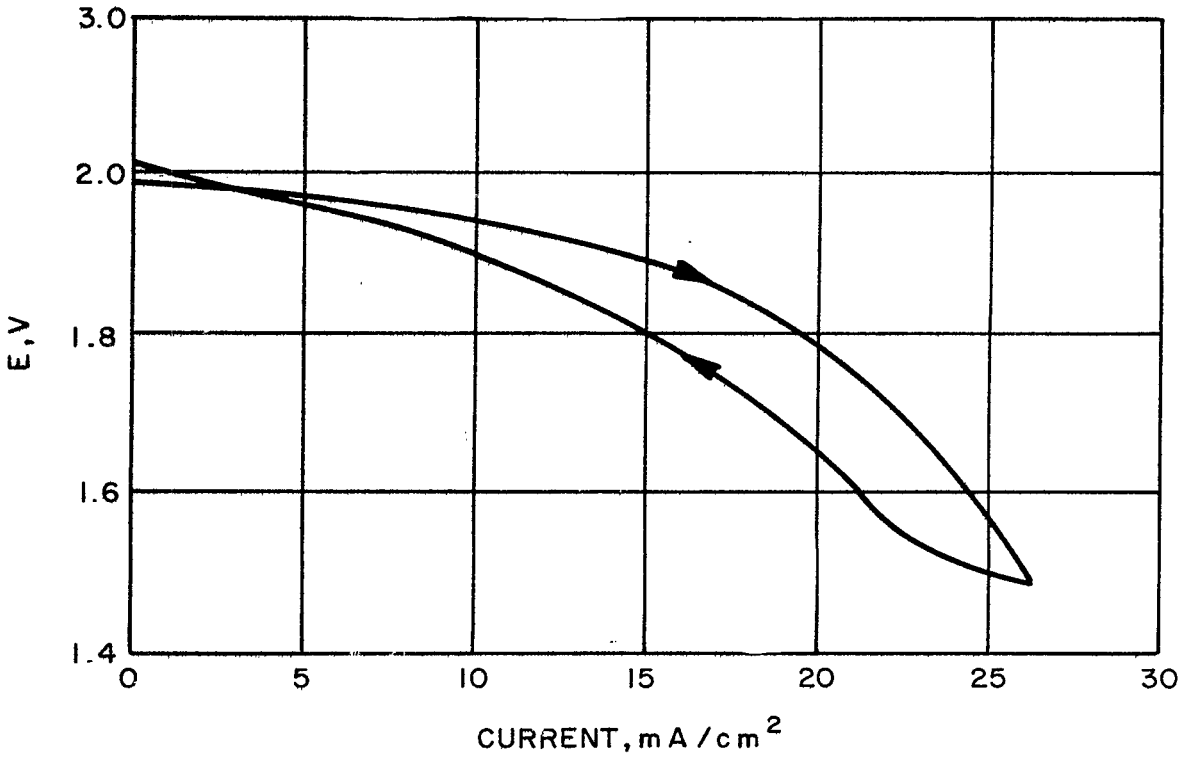

Fig. 25. Stationary current-voltage behavior of experimental Al-Cl cell (porous Speer carbon no. 37 electrode; Cl_2 pressure = 10 psig; $AlCl_3$-KCl-NaCl = 66-14-20 mol %)

REFERENCES

(1) Grothe, H.: Z. Elektrochem., 53, 1949, pp. 362-9.

(2) Fischer, W. and Simon, A.: Z. Anorg. Allg. Chem., 306, 1960, pp. 1-12.

(3) Midorikawa, R.: J. Electrochem. Soc. Japan, 23,1955, pp. 127-9.

(4) Grothe, H. and Piel, C. A.: Z. Elektrochem., 54, 1950, pp. 210-5.

(5) Delimarskii, Yu. K., Berenblyum, L. S., and Sheiko, I. N.: Zh. Fiz. Khim, 25, 1951, pp. 398-403.

(6) Midorikawa, R.: J. Electrochem. Soc. Japan, 24, 1956, pp. 23-7.

(7) Midorikawa, R.: J. Electrochem. Soc. Japan, 23, 1955, pp. 72-6.

(8) Grothe, H.: Z. Elektrochem., 54, 1950, pp. 216-9.

(9) Midorikawa, R.: J. Electrochem. Soc. Japan, 23, 1955, pp. 352-5.

(10) Moss, R. H.: U. Microfilms, Ann Arbor, Mich., 64 pp., publ. no. 12, 730, Dissertation Abs., 15, 1955, p. 1325.

(11) Morozov, I. S. and Simonich, A. T.: Zh. Neorg. Khim., II, 8, (Engl. pp. 311-21), 1957, pp. 1906-14.

(12) Kryagova, A. I.: J. Gen. Chem. USSR, 9.

(13) Yamaguti, Y. and Sisido, S.: J. Chem. Soc. Japan, 62, 1941, pp. 304-7.

(14) Morozov, I. S., Korshunov, B. G., and Simonich, A. T.: Zh. Neorg. Khim., 1, 1956, pp. 1646-57. J. Inorg. Chem. USSR, 1, 1956, pp. 203-14.

(15) Plotnikov, V. A. and Kalita, P. T.: J. Russ, Phys. Chem. Soc., 62, 1930, pp. 2195-202.

(16) Chao, T.: U. Microfilms, Ann Arbor, Mich., 294 pp., publ no. 3704, Dissertation Abs., 12, 1952, p. 459.

(17) Morozov, I. S. and Tsegledi, L.: Zh. Neorg. Chim., 6, 1961, pp. 2766-75. J. Inorg. Chem. USSR, 6, 1961, pp. 1397-1402.

(18) Midorikawa, R.: J. Electrochem. Soc. Japan, 24, 1956, p. 83.

(19) Glemser, O. and Kleine-Weischede, K.: Leibigs Ann. Chem., 659, 1962. p. 17.

(20) Verdieck, R. G. and Yntema, L. F.: J. Phys. Chem., 46, 1942, p. 344.

(21) Munday, T. C. F. and Corbett, J. D.: Inorganic Chemistry, 5, 1966, 1. 1263.

(22) Verdieck, R. G. and Yntema, L. F.: J. Phys. Chem., 46, 1942, p. 344.

(23) Plotnikov, V. A., Kirichenko, E. J., and Fortunatov, N. S.: Zap. Inst. Khim. Akad. Nauk. Ukr. R. S. R., 7, 1945, p. 159.

(24) Letisse, G. and Tremillon, B.: J. Electroanal. Chem., 17, 1968, p. 387.

(25) Swinkels, D. A. J.: J. Electrochem. Soc., 113, 1966, p. 6.

(26) Will, F.: J. Electrochem. Soc., 110, 1963, p. 145.

NASA-Langley, 1970 —— 3 CR-1541

"The aeronautical and space activities of the United States shall be conducted so as to contribute . . . to the expansion of human knowledge of phenomena in the atmosphere and space. The Administration shall provide for the widest practicable and appropriate dissemination of information concerning its activities and the results thereof."

— NATIONAL AERONAUTICS AND SPACE ACT OF 1958

NASA SCIENTIFIC AND TECHNICAL PUBLICATIONS

TECHNICAL REPORTS: Scientific and technical information considered important, complete, and a lasting contribution to existing knowledge.

TECHNICAL NOTES: Information less broad in scope but nevertheless of importance as a contribution to existing knowledge.

TECHNICAL MEMORANDUMS: Information receiving limited distribution because of preliminary data, security classification, or other reasons.

CONTRACTOR REPORTS: Scientific and technical information generated under a NASA contract or grant and considered an important contribution to existing knowledge.

TECHNICAL TRANSLATIONS: Information published in a foreign language considered to merit NASA distribution in English.

SPECIAL PUBLICATIONS: Information derived from or of value to NASA activities. Publications include conference proceedings, monographs, data compilations, handbooks, sourcebooks, and special bibliographies.

TECHNOLOGY UTILIZATION PUBLICATIONS: Information on technology used by NASA that may be of particular interest in commercial and other non-aerospace applications. Publications include Tech Briefs, Technology Utilization Reports and Notes, and Technology Surveys.

Details on the availability of these publications may be obtained from:

SCIENTIFIC AND TECHNICAL INFORMATION DIVISION

NATIONAL AERONAUTICS AND SPACE ADMINISTRATION

Washington, D.C. 20546